

**UNCLASSIFIED**

---

---

**AD 284 018**

---

*Reproduced  
by the*

**ARMED SERVICES TECHNICAL INFORMATION AGENCY  
ARLINGTON HALL STATION  
ARLINGTON 12, VIRGINIA**



---

---

**UNCLASSIFIED**

NOTICE: When government or other drawings, specifications or other data are used for any purpose other than in connection with a definitely related government procurement operation, the U. S. Government thereby incurs no responsibility, nor any obligation whatsoever; and the fact that the Government may have formulated, furnished, or in any way supplied the said drawings, specifications, or other data is not to be regarded by implication or otherwise as in any manner licensing the holder or any other person or corporation, or conveying any rights or permission to manufacture, use or sell any patented invention that may in any way be related thereto.

284 018

62-4-6

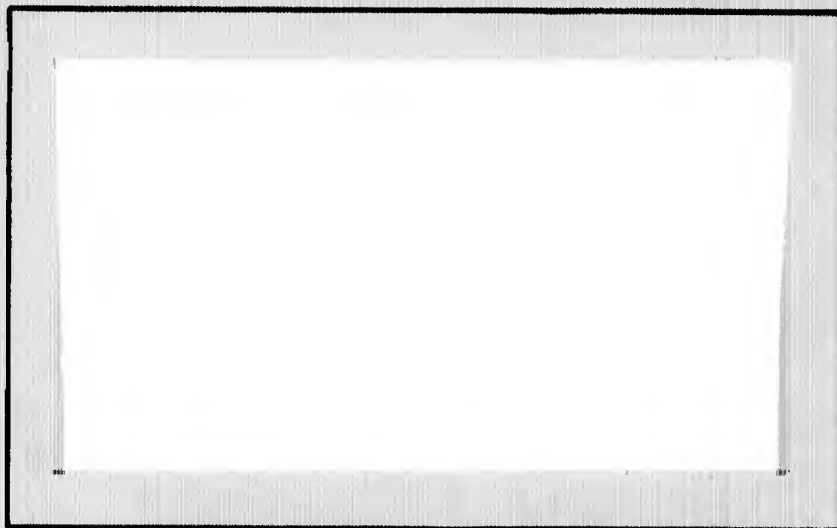
284018

CATALOGED BY ASTIA  
AS AD No. \_\_\_\_\_

# AIR FORCE INSTITUTE OF TECHNOLOGY



AIR UNIVERSITY  
UNITED STATES AIR FORCE



## SCHOOL OF ENGINEERING

WRIGHT-PATTERSON AIR FORCE BASE, OHIO

ASTIA  
RECEIVED  
SEP 20 1962  
RECEIVED  
TISIA

THE DISPLACEMENT OF THE SELENIUM  
ATOM IN SINGLE-CRYSTAL ZINC  
SELENIDE BY ELECTRON BOMBARDMENT

Captain Robert M. Detweiler

GNE/Phys/62-5

**THE DISPLACEMENT OF THE SELENIUM ATOM  
IN SINGLE-CRYSTAL ZINC SELENIDE  
BY ELECTRON BOMBARDMENT**

**THESIS**

**Presented to the Faculty of the School of Engineering  
of the Institute of Technology  
Air University  
In Partial Fulfillment of the  
Requirements for the Degree of  
Master of Science**

**By**

**Robert Milan Detweiler, B. Elec. E.**

**Captain**

**USAF**

**Graduate Nuclear Engineering**

**May 1962**

Preface

This thesis is one of the products of the co-op program that has recently been added to the program of Nuclear Engineering. This program places the student in one of the laboratories at Wright Field under the supervision of a leading scientist where he will not only be able to realize some original research, but also learn to appreciate the basic problems involved in research. It was hoped that the student would be so motivated that he would contribute after graduation from the Institute to the "in-house" research of the Air Force.

I had the good fortune to be placed in the Aeronautical Research Laboratory under Dr. Bernard Kulp. Dr. Kulp is one of the leading authorities in radiation damage and is the only one in the country who is studying crystalline compounds with a low-energy electron beam. The six months that I spent under his guidance has provided the basis for several technical papers, the first of which has already been presented at the American Physical Society Conference in Baltimore in March 1962. Dr. Kulp gave freely of his time, personally guiding my thesis research as well as patiently teaching me the rudiments of Solid State Physics. I could not have hoped to have had a better arrangement or a more interesting experience in a laboratory.

The field of radiation damage, especially in fluorescent crystals, is a challenging problem. There are many that are interested in its complexities, but few that will spend the time to try to solve them. Low-energy radiation damage is an excellent supplement to the high-energy particle analysis associated with Nuclear Engineering. I sincerely hope that one of the results of this paper will be to interest future students to work in this fascinating field.

Robert M. Detweiler

Contents

	Page
Preface. . . . .	ii
List of Figures. . . . .	vi
Abstract . . . . .	viii
I. Introduction . . . . .	1
Advantages of Electron Bombardment. . . . .	1
Related Work. . . . .	3
II. Some Physical and Optical Properties of Zinc Selenide . . .	5
Physical Properties of ZnSe Crystals. . . . .	5
Optical Properties . . . . .	6
Crystal Growth Characteristics . . . . .	7
Chemical Analysis . . . . .	8
III. Fundamentals of Defect Production. . . . .	10
Displacement of Atoms. . . . .	11
Effects on Fluorescence Caused by Defects. . . . .	14
IV. Experimental Procedure . . . . .	19
Approach to the Problem. . . . .	19
Generalized Bombardment Schedule. . . . .	20
V. Experimental Equipment . . . . .	22
Van de Graaff Accelerator and Associated Equipment . .	22
Cockcroft-Walton Accelerator . . . . .	27
Glass Prism Spectrometer. . . . .	28
Densitometer . . . . .	28
VI. Data and Results of Electron Bombardment of Zinc Selenide	30

	Page
Crystal Selection . . . . .	30
The Fluorescence Spectrum of ZnSe . . . . .	32
Near Infrared Spectra . . . . .	32
Spectrum in the Visible Region . . . . .	35
Discussion . . . . .	37
Displacement of the Selenium Atom . . . . .	39
Displacement Data and Results . . . . .	39
Discussion . . . . .	50
Conclusions . . . . .	55
Bibliography . . . . .	57
Vita . . . . .	59

List of Figures

Figures	Page
1 The Cross-Section for Selenium Atom Displacement as a Function of Electron Bombardment Energy . . . . .	13
2 Continuum of Energy Levels in the Band-Gap, Showing the Positions of the Lines of Demarcation and Fermi Levels for Holes and Electrons . . . . .	17
3 Van de Graaff Cryostat Showing the Location of Crystal Mounting . . . . .	23
4 Spectrometer and Associated Recording Electronics for the Van de Graaff Accelerator. . . . .	25
5a Spectral Response of the Lead Sulfide Cell . . . . .	26
5b Spectral Response of the S-11 Photomultiplier . . . . .	26
6 The Fluorescence of ZnSe in the Infrared at 77°K Excited with 300 kev, 5.0 Microamps/cm <sup>2</sup> Bombardment Electrons . . . . .	33
7 The Temperature Dependence of the Infrared Fluorescence Bands in ZnSe (Electron Excitation) . . . . .	34
8 Densitometer Traces of ZnSe Fluorescence Under X-Rays and Ultraviolet at 77°K . . . . .	36
9 ZnSe Fluorescence Under 350 kev Electrons While at Liquid Nitrogen Temperature. . . . .	40
10 ZnSe Fluorescence After 10 <sup>18</sup> Electrons at Energies Between 350 kev and 400 kev at 300°K . . . . .	42
11 ZnSe Fluorescence After 3 x 10 <sup>17</sup> Electrons at 350 kev at 77°K . . . . .	43
12 The Rate of Growth of the 0.55 Micron Band at Various Energies as a Function of Bombardment Time . . . . .	45

Figure	Page
13 The Rate of Growth of the 0.55 Micron Band as a Function of Electron Bombardment Energy. . . . .	47
14 The Fluorescence Growth of the 0.55 Micron Band Under 250 kev Electrons at Liquid Nitrogen Temperature. . . . .	48
15 The Temperature Dependence of the 0.55 Micron Band While Under 275 kev Bombardment Electrons . . . . .	49
16 Schematic Arrangement of the Interstitial Diffusion Experiment on ZnSe . . . . .	53

Abstract

The fluorescence structure and the displacement energy of lattice atoms in single-crystal synthetic zinc selenide have been investigated with a low-energy electron beam probe. Fluorescence peak intensities at 77°K have been observed at 0.45 $\mu$ , 0.46 $\mu$ , 0.49 $\mu$ , 0.525 $\mu$ , 0.55 $\mu$ , 0.64 $\mu$ , 0.85 $\mu$ , 1.0 $\mu$ , 1.25 $\mu$ , 1.65 $\mu$ , 2.0 $\mu$ , and 2.2 $\mu$ . The temperature dependence of 5 of the more prominent peaks has been examined. The structured edge emission containing as many as 5 lines has also been observed. The threshold for the controlled growth of a broad 0.55 $\mu$  peak band was observed at 240  $\pm$  10 kev, which corresponds to a maximum energy transfer to the selenium atom of 8.2 ev. Although positive evidence is lacking, the causing defect for the 0.55 $\mu$  band appears to be the selenium vacancy.

THE DISPLACEMENT OF THE SELENIUM ATOM IN SINGLE-CRYSTAL  
ZINC SELENIDE BY ELECTRON BOMBARDMENT

I. INTRODUCTION

The purpose of this work is to investigate the relationship between the displacement of atoms in the lattice of single-crystals of zinc selenide and the existence of certain bands observed in the fluorescence spectrum. The displacement of the lattice atoms was accomplished by electron bombardment, while the fluorescence spectrum was observed as a result of ionization by ultraviolet (uv), x-rays, or electrons. The definition of the displacement energy for the selenium atom from the zinc selenide crystal lattice as well as the study of the fluorescence spectrum preceding this measurement are presented.

Advantages of Electron Bombardment

Electron bombardment, as contrasted to heavy particle bombardment, provides a much more qualitative analysis of crystalline behavior. Neutron damage, for example, has been by far more intensively studied, but by the very nature of its damage little more than effect can be analyzed. In order to find the cause of crystal degradation and consequently the basic properties of its defects, radiation damage

would have to be minutely controlled even to the extent of being able to effectively account for defect ionization. Further, displacement of atoms by neutrons where there is a large transfer of momentum leads to a complex kind of damage such as formation of clusters and localized heating of the lattice, leaving the crystal in a state in which the distribution of the induced defects is nonuniform. Electrons, on the other hand, transfer a small momentum to the displaced atoms. The probability that such a displaced atom can produce further displacements is low.<sup>19</sup> One should expect, therefore, that in its simplest form, displacements by incident electrons will consist of individual vacancy-interstitial pairs called Frenkel defects. Interstitial atoms are defined as being any atom that is dislocated from the regular array of the crystal lattice. A low-energy electron beam has been used and been proven to be a very satisfactory probe for the energy measurement of these defects and for the subsequent recombination radiation and hence, a method for defect definition.

The true complexity of this program has slowly become apparent. Each class of solid that has been investigated under bombardment behaves differently, and with further study the individual members of each class have proven to be quite distinct. Thus, through radiation experiments, the noble metals copper, silver, and gold, which have

often been treated as though they were alike, have proven to be quite different. Another important factor is the ability of radiation damage to heal its own induced defects, which is termed "annealing," at extremely low temperatures. Also, one finds that individual defects will perturb one another unless levels of exposure are kept very low, but even at such low levels the influence of impurities and existing lattice defects still complicates the picture in even the most carefully prepared crystal specimens. Different kinds of radiation will cause different results, so that the control of quality and intensity of the radiation is most important.

#### Related Work

In 1957, D. C. Reynolds and L. C. Greene at the Aeronautical Research Laboratory, Wright-Patterson Air Force Base, reported they had produced green edge emission in cadmium sulfide, a II-VI compound, by proton bombardment at 1 mev.<sup>15</sup> The mechanism for this production was merely observed, but not well defined. It was decided to explore the possibility that this emission might have been caused by the displacement of either the sulfur or cadmium atom from the lattice. Dr. Bernard A. Kulp was engaged for this work and subsequently found, through the use of a low-energy electron beam probe, that this emission was due to the sulfur interstitial.<sup>10</sup> Continued

work by Dr. Kulp on this compound over the past three years using the electron beam has resulted in establishing the threshold, which is the energy for the displacement of a lattice atom, for both sulfur and cadmium,<sup>11</sup> and their effect on the near-infrared fluorescence.<sup>12</sup> The work has now expanded to other II-VI semiconductor compounds such as the sulfides, tellurides, and selenides of cadmium, zinc, and mercury.

## II. SOME PHYSICAL AND OPTICAL PROPERTIES OF ZINC SELENIDE

The properties of zinc selenide are generally known in so far as the ones that are directly associated with cathodoluminescence and electroluminescence.<sup>13</sup> The optical and fluorescent properties have only recently received enough attention to be accurately measured and even today, most of the theories associated with these measurements have not been extensively verified. The following sections present a review of some of the properties of this compound.

### Physical Properties of ZnSe Crystals

Zinc selenide is a II-VI semiconductor compound which has an interpenetrating face-centered cubic lattice with a lattice constant of  $2.8 \times 10^{-8}$  cm at 300°K. This type of lattice is often referred to as a zinc blende structure.<sup>13</sup> The macroscopic structure of the crystal, however, is not uniform. Crystals from the same preparation can vary from a very brittle opaque crust-like construction to a clear crystalline structure that can be easily cleaved. All of the various types of construction were investigated on the basis of their "as-grown" fluorescence pattern.

The color of ZnSe varies from yellow to dark red. L. C. Greene of the Aeronautical Research Lab reports that the red crystals can be

made by cooking stoichiometric proportions of Zn and Se at about 1200°C. The crystals are initially yellow in the early stages of growth, but turn a deeper red the longer they are cooked. This is most probably due to the more volatile selenium being sublimed from the crystal. This is supported by G. A. Zholdevich who reported that decreasing the selenium content in the crystal preparation was accompanied by the appearance of an extended long wavelength tail in the absorption spectrum all the way out to 1.0μ.<sup>20</sup> Thus, the red ZnSe crystals are characterized by a selenium deficiency.

The density has been measured at 5.42 gm/cm<sup>3</sup>, which gives a value of 1.13 x 10<sup>22</sup> atoms/cm<sup>3</sup>.

The value for the heat of sublimation for ZnSe has been found to be 65.0 kilocalories/mole.<sup>9</sup> From this value, the displacement energy for the selenium atom is roughly estimated to be about 11.3 ev.

### Optical Properties

The absorption edge in ZnSe has been known for quite some time. R. H. Bube measured this quantity to be 2.80 ev at 90°K. He also measured the temperature dependency by photoconductivity response between 90°K and 400°K to be

$$E(\text{ev}) = 2.80 - 0.00072 T \quad (1)$$

where T is the temperature in degrees Kelvin.<sup>4</sup> A later measurement

by Reynolds, Pedrotti, and Larson of 2.83 ev at 4.2°K confirmed the extrapolation of this dependency.<sup>16</sup> G. A. Zholdevich found the band-gap to be 2.66 ev at room temperature, which is also in close agreement.<sup>20</sup>

Absorptivity experiments by Zholdevich have shown the maximum absorptivity band to be at 4437 Å with a 0.7 Å/degree Kelvin displacement.<sup>20</sup>

Reflectivity measurements on ZnSe have been done mainly by M. Aven, et al. of General Electric Research Lab.<sup>2</sup> A number of optical constants in the 1.0 to 10 ev range were obtained. Efforts by Dr. D. Langer, ARL, to reproduce these results have been unsuccessful. Aven also made some mobility versus temperature measurements using various doping agents, but did not use a large enough temperature range to develop a good analysis.<sup>2</sup> However, the ohmic resistance limits have been found to be  $10^6$  to  $10^{12}$  ohm-cm in undoped crystals.<sup>20</sup>

#### Crystal Growth Characteristics

Zinc selenide is a covalent compound that is characterized by a loosely packed structure with large interstitial spaces in which displaced atoms or impurities may lodge.<sup>13</sup> It can be grown from the melt or vapor phase and can be made either "p" or "n" type.<sup>5</sup>

It forms solid solutions with most other II-VI compounds giving it a large variety of doping possibilities. Although there are several refined methods for the preparation of ZnSe crystals, single crystals are difficult to obtain because of the refractory nature of ZnSe and its pronounced tendency to decompose far below its melting point of  $1515^{\circ}\text{C}$ .<sup>5</sup>

The ZnSe crystals used in this experiment were grown at ARL by controlled zone-sublimation-recrystallization method developed by Greene, Reynolds, and Czyzak.<sup>7</sup> Such vapor phase growth, as opposed to melt growth, has fewer native dislocations because of two basic reasons; first, vapor phase growth takes place at a lower temperature and secondly, the ingredients are never in the liquid phase so generally there are no stoichiometric gradients or impurity segregations.<sup>5</sup>

#### Chemical Analysis

In our experiments crystals from two separate preparations were used. The first run produced yellow crystals of various sizes and construction that were cleaned and ground as needed. Although the crystals were not intentionally doped, spectrochemical analysis showed copper, silicon, magnesium, and calcium present in quantities of about 0.001% and silver, manganese, aluminum and iron in quantities of 0.0001%.

Crystals produced from the second run were of uniform crystalline construction and were a dark red. These crystals could be easily cleaved so almost no grinding was necessary in their preparation. They also were undoped, but their chemical analysis showed impurities of silicon, magnesium, manganese, beryllium, iron, chromium, calcium and silver in quantities of less than 0.001% and copper in a quantity of less than 0.01%

### III. FUNDAMENTALS OF DEFECT PRODUCTION

The interaction of energetic electrons with matter is a rather complex phenomena and it is useful to reduce this process to two categories based on effect rather than cause. The primary or direct effects consist of ionization of host atoms and defects, the displacement of atoms from lattice sites, excitation of atoms without displacement, interorbital electron excitation, and the transmutation of nuclei. Transmutation takes place in the energy range of several mev, which is far above the electron energies of this experiment. Interorbital electron excitation of tightly bound states results in Auger electrons which cause further ionization, x-ray emission, or characteristic fluorescence. Valence electrons are generally excited into the conduction band and this process can be classed as ionization. Atom excitation without displacement is dissipated by lattice vibrations and thermal ionization, which may or may not be radiative. The displacement of atoms is the object of this experiment, while fluorescence resulting from ionization of valence band and defect atom electrons provides the means by which displacement is observed. These two phenomena, displacement and fluorescence, will now be discussed.

Displacement of Atoms

In radiation damage considerations, the most important characteristic of a collision is the energy transferred to the struck atom. This may range from zero in glancing collisions to a maximum,  $T_m$ , which is transferred in a head-on collision. Since the fluorescence is very sensitive to defect population, the energy at which displacements are first produced is most important. In a classical consideration of energy and momentum conservation it is easily seen that

$$T_m = \left[ \frac{4 m_1 M_2}{(m_1 + M_2)^2} \right] E \quad (2)$$

where  $m_1$  is the electron mass,  $M_2$  is the struck atom mass, and  $E$  is the electron energy.<sup>18</sup> Using 240 kev as the electron bombardment energy necessary to displace selenium,  $T_m$  is 6.6 ev. However, the case of electron bombardment requires some modification of (2).

Because of the small mass of the electron, it must travel at relativistic velocities in order to produce displacements, Formula (2) now becomes

$$T_m = \frac{2 \left[ E + 2 m_1 c^2 \right] E}{M_2 c^2} \quad (3)$$

where  $c$  is the velocity of light.<sup>18</sup> Relativistic considerations change  $T_m$  to 8.2 ev. This value from collision theory is somewhat smaller

than 11.3 ev obtained from the heat of sublimation.

The probability that a given amount of energy will cause a displacement can be measured in terms of a small area through which the electron must pass in order for this energy transfer to occur. If it is assumed that a selenium atom is always displaced when it receives energy greater than its threshold energy and is never displaced at lower energies, the total cross-section for production of the selenium interstitial is

$$\sigma_d = 16 \pi a_0^2 Z_2^2 \left[ \frac{m_1^2}{(m_1 + M_2)^2} \right] \frac{E_r^2}{T_m^2} \left[ \frac{T_m}{E_d} - 1 \right] \quad (4)$$

where  $a_0$  is the Bohr radius,  $Z_2$  is the selenium atomic number and  $E_r$  is the Rydberg energy constant.<sup>18</sup> The total cross-section rises steeply from zero at the threshold energy and then becomes constant as the bombardment energy increases. This equation applies for  $T_m$  between  $E_d$ , the atom displacement energy, and about  $2 E_d$ , where equation (3) is used to calculate  $T_m$ . For  $T_m$  much larger than  $E_d$ , the cross-section in the limit approaches

$$\sigma_c = \frac{8 \pi a_0^2 Z_2^2 E_r^2}{M_2 c^2 E_d} \quad (5)$$

The calculated value of  $\sigma_c$  has a value of 246 barns.<sup>18</sup> Figure 1

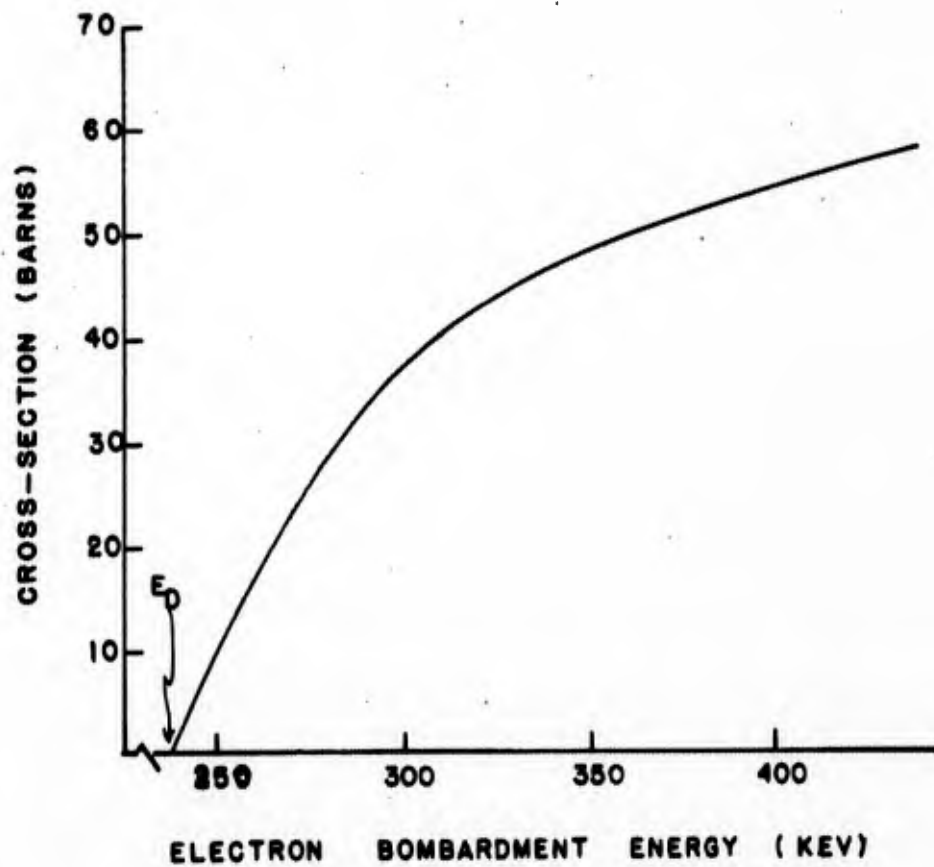


FIGURE 1: THE CROSS-SECTION FOR SELENIUM ATOM DISPLACEMENT AS A FUNCTION OF ELECTRON BOMBARDMENT ENERGY

shows the cross-section as a function of electron bombardment energy.

#### Effects on Fluorescence Caused by Defects

Most of the energy of the electron beam is dissipated in ionization of crystal host atoms and defects. It is reasonable to assume that multiple-ionized states of defect and host atoms can exist each having their own fluorescent properties. Any radiation capable of producing ionization can therefore change the population of the energy states of a defect thereby causing a redistribution of electrons over existing defects. Any or all of these states are interchangeable under ionizing radiation and may or may not take part in recombination, so that one might observe the growth or decline of a particular fluorescence band solely due to ionization of a defect. Thus, such a growth or decline would result from a change in the relative population of ionized states and therefore would generally not exhibit any threshold property.

The total number of electrons in the conduction band increases as a result of ionization. This number is also a function of the temperature since temperature increases cause increased lattice vibrations which can thermally ionize electrons from shallow traps. The transition of an electron to its ground state would clearly be a function of the number of electrons and defect recombination centers, temperature,

as well as a distinct probability factor that such a transition can take place. Not all the conduction electrons are free to recombine, some being trapped at various energy levels in the band-gap. The energy position under equilibrium conditions in the band-gap where there is a 50% probability of trap occupation is called the Fermi Level. Consequently, this level would be dependent on any factor that changes the number of ionized electrons or the total defect population.

The Fermi Level differs among undoped crystals since it is dependent on minute defects which are insensitive to chemical analysis. These defects tend to collect on surfaces, flaws, or boundary layers in the crystal. Thus the Fermi Level and the fluorescent spectra from different sections of the same crystal are frequently not the same.<sup>1</sup> New defects, under bombardment, are randomly created in a crystal. The position of the energy levels of these defects in the band-gap will determine a shift in the various Fermi Levels and consequently an overall change in the recombination probabilities. Such a shift may lessen the probability for that center participating in a radiative recombination as well as enhance it. Therefore, defect production is not always accompanied by a fluorescence band growth.

Under excitation it is not appropriate to define a Fermi Level since there no longer exists a Fermi distribution of electron energy.

According to the model proposed by A. Rose,<sup>17</sup> the Fermi Level splits into two separate energy levels which he calls the Fermi Level for electrons,  $E_{fe}$ , and the Fermi Level for holes,  $E_{fh}$ . These two levels are defined on the basis of 50% trap occupation, except  $E_{fe}$  is concerned only with electron densities and  $E_{fh}$  with hole densities. Figure 2 shows the location of these levels under the influence of electron bombardment.

A second set of energy lines shown in Figure 2 are termed lines of demarcation. Electrons in shallow traps near the conduction band generally do not take part in recombination since they are very easily ionized. The line of demarcation for electrons,  $L_e$ , is that energy position in the band-gap where the probability of a trapped electron capturing a free hole becomes greater than its probability for reionization. The line of demarcation for holes,  $L_h$ , is defined in the same manner. One may conclude from these definitions that the recombination of electrons and holes is chiefly determined by the centers that lie between the demarcation lines. Under heavy ionization, such as electrons or x-rays, there would be a shift of both lines of demarcation toward the conduction band but not necessarily the same increment for both. This in turn would change the probabilities of an electron being trapped at or below the electron demarcation line and thus

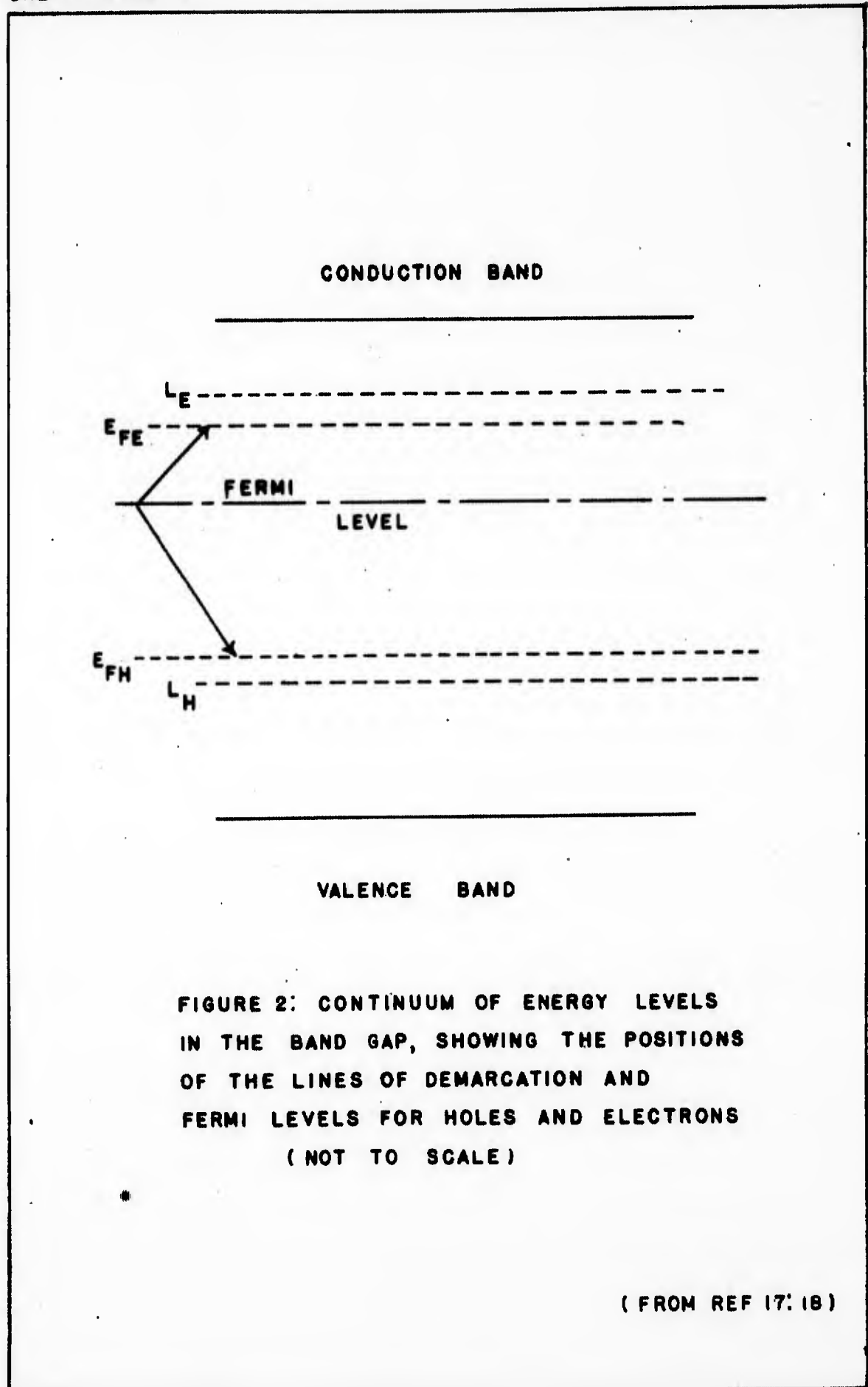


FIGURE 2: CONTINUUM OF ENERGY LEVELS IN THE BAND GAP, SHOWING THE POSITIONS OF THE LINES OF DEMARCATION AND FERMI LEVELS FOR HOLES AND ELECTRONS (NOT TO SCALE)

( FROM REF 17: 18 )

improve its chances for transition to its ground state. Under a less energetic source, such as ultraviolet light, the demarcation lines would move less radically thus affecting recombination to a smaller degree. An energy level within a few  $kT$  above the electron demarcation line would change from a reionizing level to a recombination center under heavy ionization, but would most likely remain a reionizing level under less intense radiation. Thus, this model affords a plausible explanation of fluorescent spectra that are dependent on the source of excitation.

IV. EXPERIMENTAL PROCEDUREApproach to the Problem

Radiation damage in II-VI compounds is observable through changes in their fluorescent spectra. Since the spectrum of ZnSe was largely unknown, with the exception of the region near the band edge, the fluorescence was examined from the band edge to about  $2.4\mu$ , the limit of this laboratory's equipment. This examination was done at room temperature and at liquid nitrogen temperature ( $77^{\circ}\text{K}$ ) since nearly all the fluorescent lines of ZnSe appear at these temperatures. The fluorescence was observed under three different sources of excitation. X-rays were used to excite the visible fluorescence to overcome the lack of intensity with ultraviolet. Band-gap light was used for the infrared region to preclude interference by the mercury spectrum and to exclude x-ray shielding problems. Electron excitation was used to provide a means to observe these fluorescent regions as well as a means to induce radiation damage.

The displacement experiments were done with the electron beam. An electron accelerator in conjunction with a spectrometer was used to observe changes in the fluorescence pattern of ZnSe as a result of the production of crystal defects. The following generalized bombardment sequence shows a method for defining this phenomena.

Generalized Bombardment Schedule

The fluorescence of an "as-grown" crystal is first excited by one of the above methods and analyzed. Subsequent electron bombardment is then carried out in energy regions based on classical calculations of energy transfer and heat of sublimation of ZnSe. The fluorescence is followed as a function of bombardment time. As the electron energy is changed through these displacement regions, one hopefully looks for a fluorescent band that will grow beyond a certain energy and will remain stable or decrease when the electron energy is below that value. If such a band proves to be controllable, so that it can be grown or destroyed under a given set of conditions, then one expects a correlation between the fluorescent band and the crystal damage at that energy.

It is a well accepted fact that crystal defects are responsible for the various fluorescent patterns in ZnSe.<sup>19</sup> To differentiate between interstitials, vacancies, and combinations of these, overlay experiments such as those on CdS can be tried.<sup>10, 11</sup> This is done by evaporating a thin layer of one of the constituents of the compound onto a portion of the crystal; the remaining part is masked off to prevent deposit. The crystal is subsequently bombarded through the overlay so that the atoms of the overlay are driven down into the crystal by the incident electrons. This is done below the threshold energy for the

production of the suspect interstitial atom from the crystal. If the fluorescence band appears on the unmasked section, one can strongly speculate a fluorescence band-interstitial relationship. If the particular band does not appear, the causing defect can most likely be associated with the vacancy. Densitometer traces of glass prism spectrometer pictures of the fluorescence can be used to verify any fluorescence change.

The successful conclusion of this sequence does not offer conclusive proof of a defect-fluorescence band relationship since a change in defect population or their states of ionization may occlude or enhance this fluorescence. However, the overlay effect reproduced in a number of crystals combined with a well defined fluorescence band threshold provides a necessary, if not a sufficient condition, for the production of the particular defect.

## V. EXPERIMENTAL EQUIPMENT

Crystal bombardment was carried out with two electron accelerators. The resulting fluorescence was analyzed with a spectrometer fitted with a photomultiplier and/or lead sulfide cell in conjunction with an X - Y or strip-chart recorder. The fluorescence spectra were also recorded on film of various sensitivity and wavelength response with x-rays and ultraviolet as the means of excitation. In the following discussion each system is described in detail.

### Van de Graaff Accelerator and Associated Equipment

Electrons have an energy range of about 150 kev to 1.0 mev in this machine. The range which was used in this experiment was 175 kev to 500 kev at a steady electron d. c. current of  $5\mu\text{a}/\text{cm}^2$ . The electron energy was calibrated at 300 kev with aluminum foil of  $0.010 \pm 0.0005$  inches thickness mounted in front of an anthracene scintillation crystal. Extrapolated penetration of electrons gave a maximum range of  $0.081 \text{ gm}/\text{cm}^2$  as compared with about  $0.082 \text{ gm}/\text{cm}^2$  from R. D. Evans,<sup>6</sup> which gives an electron energy error of not more than  $\pm 5\%$ . Crystals were mounted with a conducting cement (General Cement Silver Paint) on a copper finger extending from a cryostat as shown in Figure 3. This arrangement facilitated temperature control during bombardment from  $77^\circ\text{K}$  to room temperature. In

1 INCH

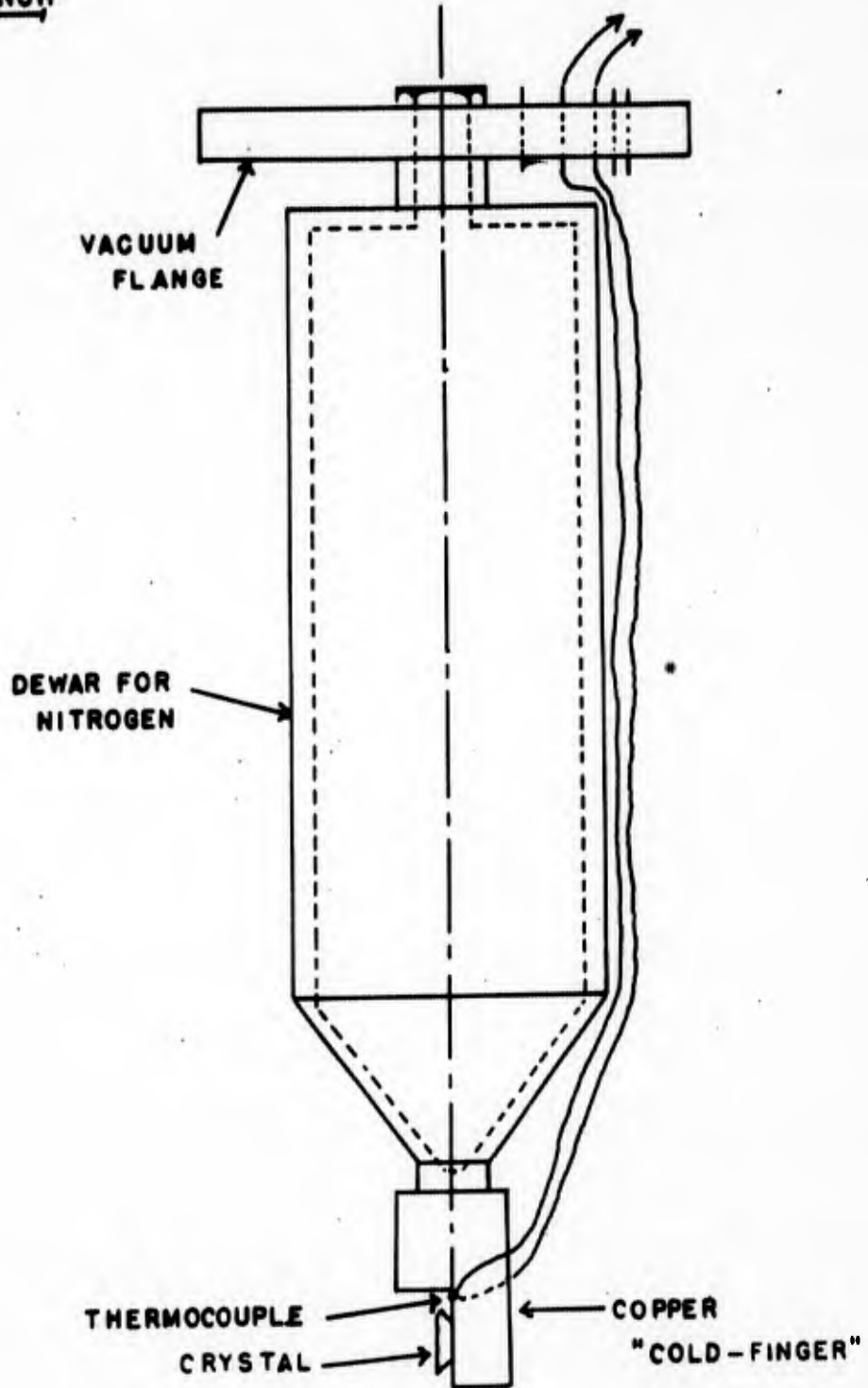


FIGURE 3: VAN DE GRAEFF CRYOSTAT  
SHOWING THE LOCATION OF CRYSTAL MOUNTING

some instances heating rods were used to extend this range to  $500^{\circ}\text{K}$ . As shown in Figure 3, the cryostat can be equipped with a copper-constantan thermocouple so that crystal temperatures within  $\pm 5^{\circ}\text{K}$  can be recorded. The cryostat is placed inside the Van de Graaff so that bombardment is generally done in a vacuum of  $10^{-5}$  millimeters of mercury or less. By removal of the cryostat, crystals could be mounted outside of the evacuated chamber behind an aluminum window and bombardment carried out in atmospheric conditions.

The crystal fluorescence was diffracted by a Perkin-Elmer spectrometer equipped with a type "O" Kodak lead sulfide cell operated at 45 d. c. volts bias or a RCA 5819, S-11 photomultiplier. Figure 4 shows the schematic of this arrangement. The spectral response of the two detectors is shown in Figure 5. The lead sulfide cell has a satisfactory response between  $0.6\mu$  and  $2.7\mu$  with peak sensitivity at  $2.0\mu$ , while the photomultiplier's useful wavelength response is between  $0.35\mu$  and  $0.60\mu$ . Thus the spectrum can effectively be covered from  $0.4\mu$  to  $2.7\mu$ .

The intensity of the spectrum as seen by these two detectors was recorded by a Moseley Autograf Two Axis Recorder. Its input signal from the photomultiplier was passed through a Keithley electrometer fitted with a decade shunt to give a greater range of intensity plot.

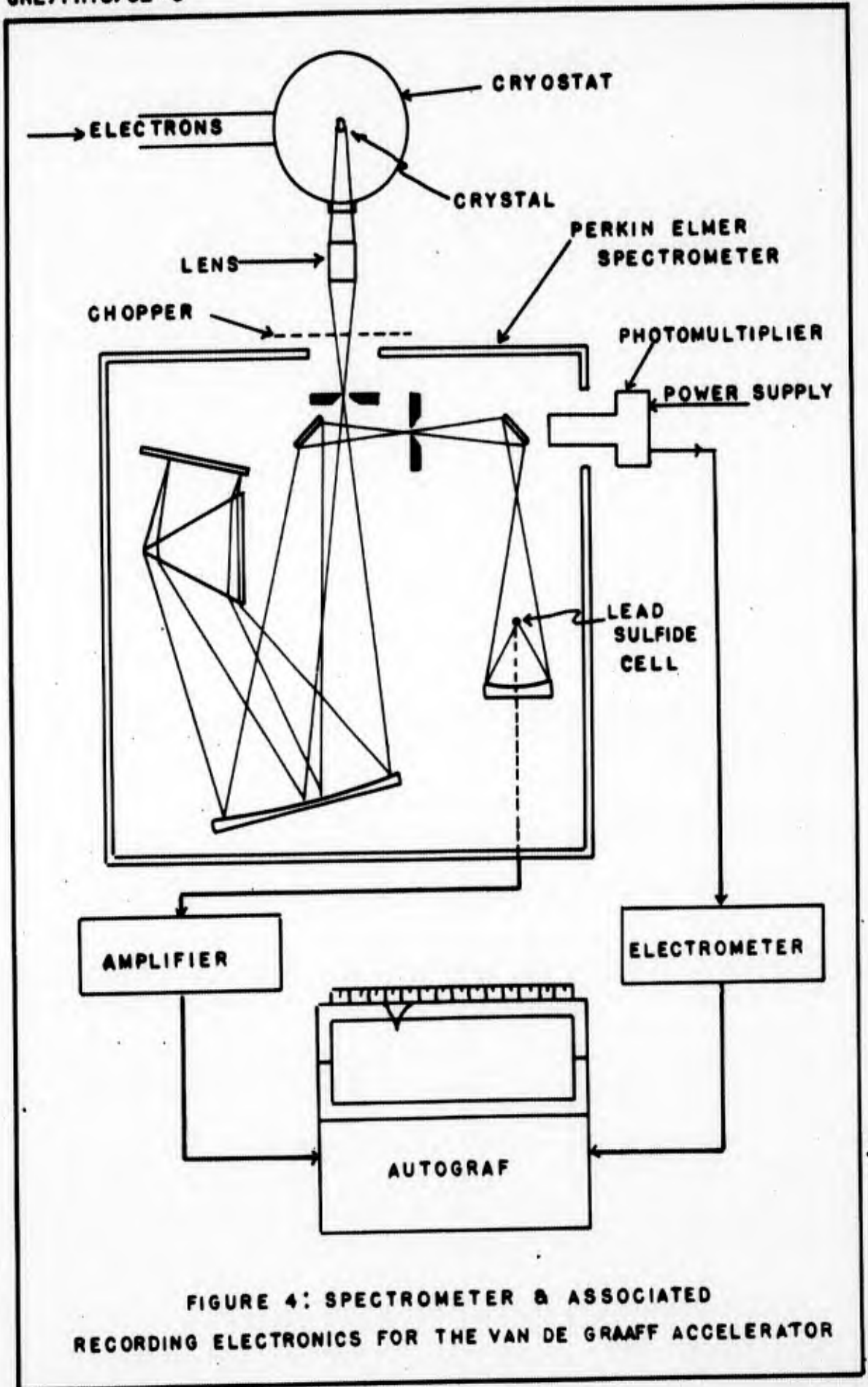


FIGURE 4: SPECTROMETER & ASSOCIATED RECORDING ELECTRONICS FOR THE VAN DE GRAAFF ACCELERATOR

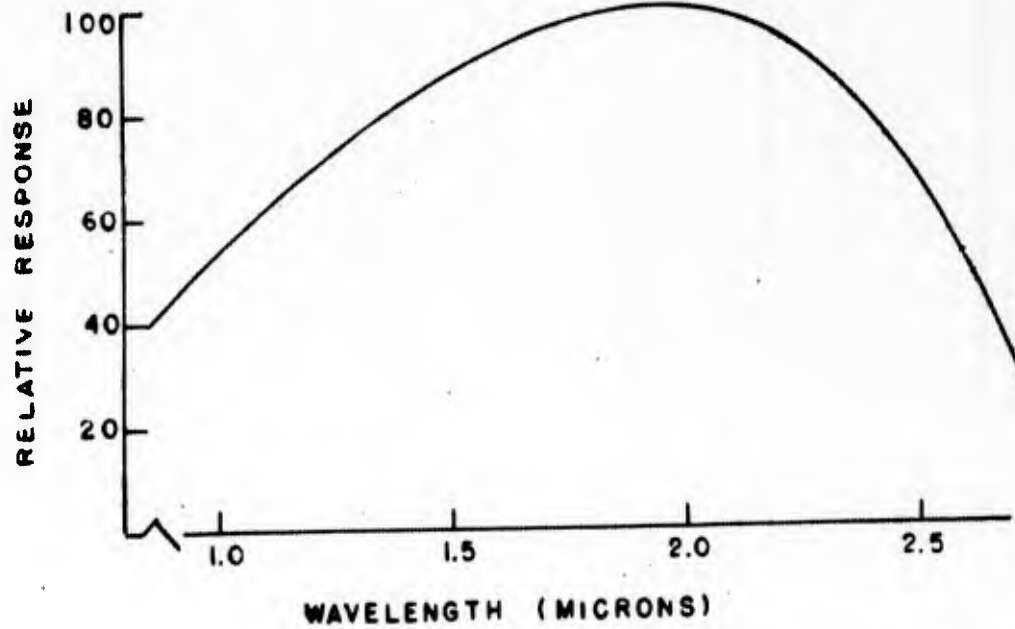


FIGURE 5A: SPECTRAL RESPONSE OF THE LEAD SULFIDE CELL

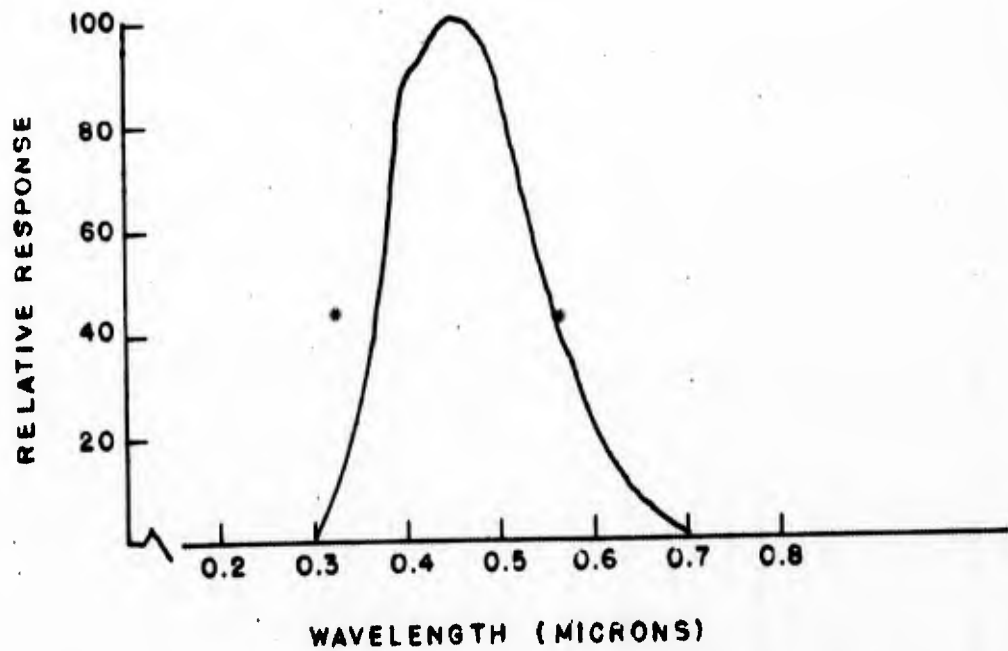


FIGURE 5B: SPECTRAL RESPONSE OF THE S-II PHOTOMULTIPLIER

When the lead sulfide cell was used, the fluorescence was chopped at 13 cycles per second. The detector signal was then amplified by an a. c. thermocouple amplifier, model 81, rectified, and fed into the Autograf. Wide range of intensity response was possible by varying the amplifier sensitivity and/or the Autograf amplitude scale.

The temperature dependence of the spectrum peaks was recorded on two of the three channels of a Micromax strip recorder, while the third channel was utilized for the temperature readout from a copper-constantan thermocouple located either in the inner Dewar of the cryostat or mounted directly on the copper finger holding the crystal.

The Perkin-Elmer spectrometer and Autograf were also used for the study of fluorescence stimulated by band-gap light. The source light was a Sylvania zirconium arc light with a  $\text{CuSO}_4$  filter placed between the arc lamp and the crystal and a Corning type 2030 filter between the crystal and the spectrometer.

This arrangement of the Van de Graaff and its associated equipment gave excellent reliability for over 800 hours of crystal bombardment.

#### Cockcroft-Walton Accelerator

The Cockcroft-Walton Accelerator was used for low-energy bombardments at  $77^\circ\text{K}$  or at room temperature. Bombardments were

carried out exclusively in a vacuum of  $2 \times 10^{-5}$  millimeters of mercury or less using electrons ranging in energy from 10 kev to 175 kev and beam currents of 2 to  $6 \mu\text{a}/\text{cm}^2$ . The crystal fluorescence was generally followed visually during bombardment, however, most any readout recording system could be used. The dependability of this machine is indicated by the fact that 520 hours of bombardment was obtained in this experiment without any maintenance trouble.

#### Glass Prism Spectrometer

This spectrometer, used in taking film pictures, was designed and fabricated by Dr. Kulp and has a useful wavelength range of about  $0.2\mu$  to  $0.7\mu$ . This apparatus was arranged so that either x-rays from a tungsten target, FA 60 type x-ray tube or ultraviolet from a H-100; SP4 tube could be used as a means of crystal excitation while at  $77^\circ\text{K}$  or at room temperature. Kodak Type I F, Type 103a F, and Type III F were used in this experiment. Types I F and 103a F are extremely fast, while Type III F has a much lower response requiring exposures four times as long as the other two type films. All three types have a maximum sensitivity range from  $0.46\mu$  to  $0.68\mu$ .

#### Densitometer

An NSL (National Spectrographic Laboratories, Inc.) Spec

GNE/Phys/62-5

Recorder, designed for spectral analysis, coupled with a Bristol strip-recording potentiometer was used to transfer spectral intensities from film to paper for ease of graphic display of fluorescence intensity. This densitometer has a variable sensitivity so that the spectral transfers show only relative intensity rather than absolute intensity.

## VI. DATA AND RESULTS OF ELECTRON BOMBARDMENT OF ZINC SELENIDE

The experimental information presented in this section points out the manner in which crystals were initially examined, the fluorescence band patterns of the selected crystals, and the definition of a defect-fluorescence relationship in ZnSe. Corrections of the data curves for lead sulfide cell response have not been applied since these corrections do not change the peak values or the shape of the bands. However, all curves from the phototube have been corrected for tube response. Although this correction does not change any peak values, the shape of the curves, especially in the longer wavelengths, is greatly affected. The argument is based on relative sizes of the peaks as well as their growth rates, which are evident on the original curves, but obviously so on the corrected ones.

### Crystal Selection

Zinc selenide has a variety of fluorescent colors. The general classes of fluorescence can be divided into four groups; blue, green, yellow, and red. These colors were not only seen singly, but in various combinations that resulted in nearly all shades of color from dark blue to a very dark red.

Ultraviolet, x-rays, and band-gap light were used to stimulate this

emission for crystal selection. Initially, only uv was used, but only very few crystals were found that fluoresced intensely enough for spectrum analysis. However, when the crystals were broken the new edges fluoresced brightly. X-rays, on the other hand, increased the intensity by at least an order of magnitude in nearly all crystals. Therefore, since spectroscopy is enhanced by intensity and since a cross-section fluorescence is desirable, x-rays at 45 kv, 40 ma at a distance of about 3 cm from the crystal were used in place of uv. X-rays at this energy have a half-thickness attenuation of about  $4 \times 10^{-4}$  cm while uv penetrates a total distance of about  $10^{-5}$  cm.

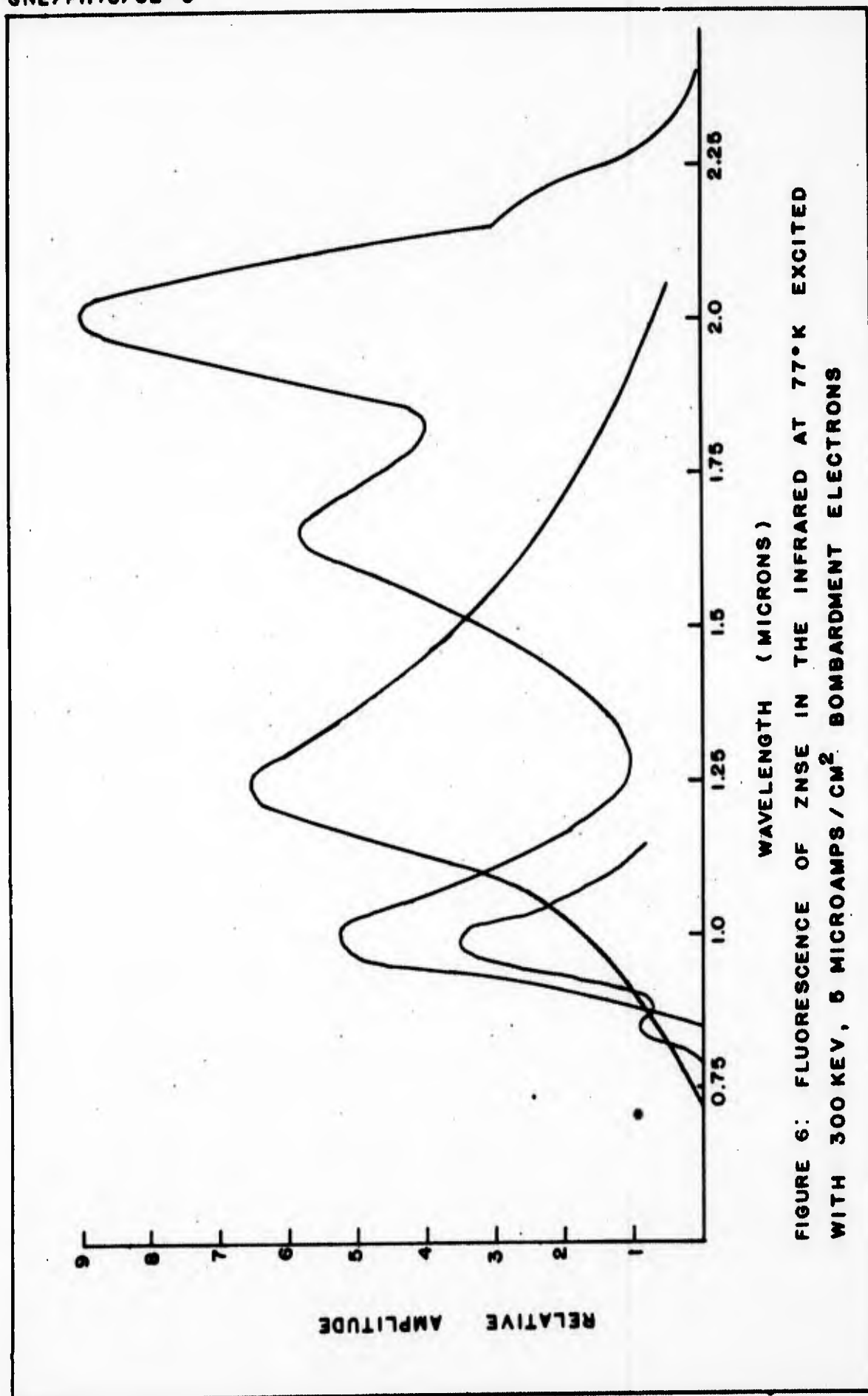
Crystals from the second preparation fluoresced red or yellow at  $300^{\circ}\text{K}$  or  $77^{\circ}\text{K}$  under uv or x-rays. The yellow fluorescence increased in intensity as it was cooled, while the red sometimes shifted to yellow. Under x-rays at  $77^{\circ}\text{K}$ , there was always an increase in intensity, especially notable with the yellow. However, a green layer was observed on the red fluorescing crystals on the side closest to the x-ray beam. This could possibly be attributed to an increase in the ionization density in the first increment of the crystal.

Yellow crystals from the first preparation were used almost exclusively throughout the experiment. These crystals were separated under x-rays at  $77^{\circ}\text{K}$  into those which fluoresced blue, those which fluoresced green, and those showing essentially no fluorescence.

The Fluorescence Spectrum of ZnSe

The fluorescence of ZnSe in the visible region has been studied by several investigators.<sup>9,13,16</sup> With the exception of work by Avinor and Meijer<sup>3</sup> on vanadium activated ZnSe, little reference is made to observations in the infrared region of the spectrum. The fluorescence spectra of several ZnSe single crystals is described as well as the temperature dependence and dependence on stimulating radiation of some of these fluorescence bands.

Near Infrared Spectra. Figure 6 shows the spectrum of several ZnSe crystals at 77°K under electron excitation at 300 kev,  $5.0\mu\text{a}/\text{cm}^2$ . The fluorescence peaks at about 0.85 $\mu$ , 1.00 $\mu$ , 1.25 $\mu$ , 1.65 $\mu$ , 2.0 $\mu$ , and 2.2 $\mu$  are observed. At 300°K only the 2.0 $\mu$  and sometimes the 2.2 $\mu$  bands are observed. Figure 7 shows the temperature dependence of the most prominent bands in the range of 77°K to 300°K. The three shorter wavelength bands decrease monotonically as the temperature is increased. The 2.0 $\mu$  band however, reaches a maximum at about 175°K. There is some variation in the temperature dependence of the 1.65 $\mu$  band which is seen at 300°K in some crystals. Neither the 1.0 $\mu$ , the 0.85 $\mu$ , nor the 1.25 $\mu$  bands have been observed at 300°K. All of these bands are observed when the crystal is excited with band-gap light except that the intensity of the 2.0 $\mu$  band is generally much less



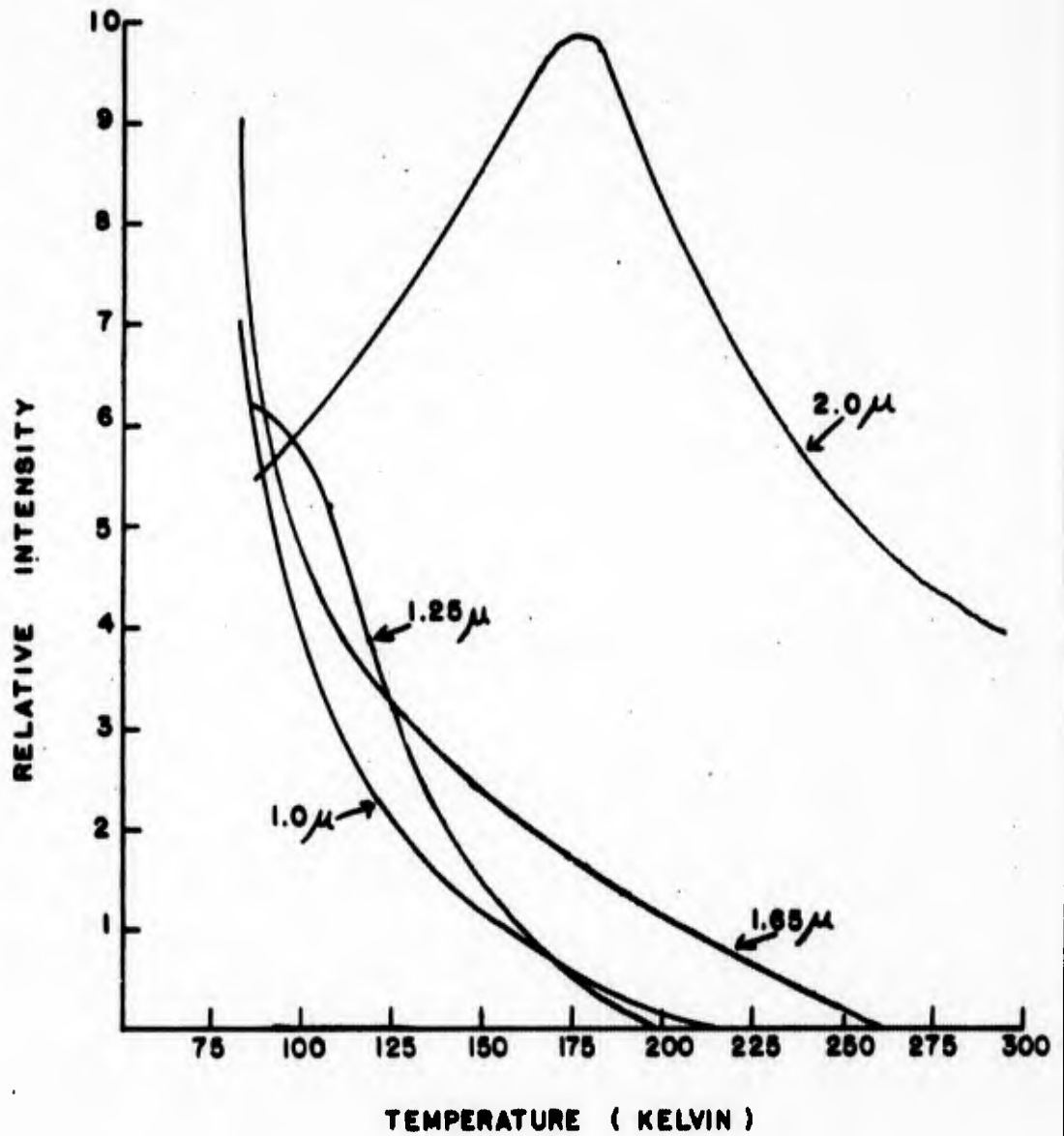


FIGURE 7: THE TEMPERATURE DEPENDENCE OF THE INFRARED FLUORESCENCE BANDS IN ZNSE (ELECTRON EXCITATION)

at 77°K compared to its intensity at 300°K. It should be noted that the relative intensities of bands vary from crystal to crystal and that any or all of the bands may be absent or present in different crystals.

The origin of these bands is uncertain, but since the doping is accidental, it is probable that some of them originate from defects in the crystals, e.g., vacancies, interstitials, and/or combinations of these with impurities.

Spectrum in the Visible Region. Noticeable differences are observed in the visible fluorescence spectra when the crystals are excited with uv and x-rays or electrons. X-rays or electrons stimulate very similar fluorescence patterns. One difference between uv and x-ray excitation is in the crystals showing a phonon structured edge emission at 77°K. In place of only two lines of the series,<sup>16</sup> when the crystal is excited by x-rays as many as five lines may be seen. The intensity is also considerably increased. The emission very near the band edge on the other hand is not usually observed under x-radiation. In many crystals a second difference is observed as shown in Figure 8. The spectrum under uv light shows broad bands at 0.49 $\mu$ , 0.525 $\mu$ , and 0.64 $\mu$ , while under x-rays the phonon structure lines at 0.458 $\mu$ , 0.463 $\mu$ , 0.468 $\mu$ , and 0.4745 $\mu$  are clearly resolved. The 0.525 $\mu$  band also appears, but with much less intensity than the structured emission.

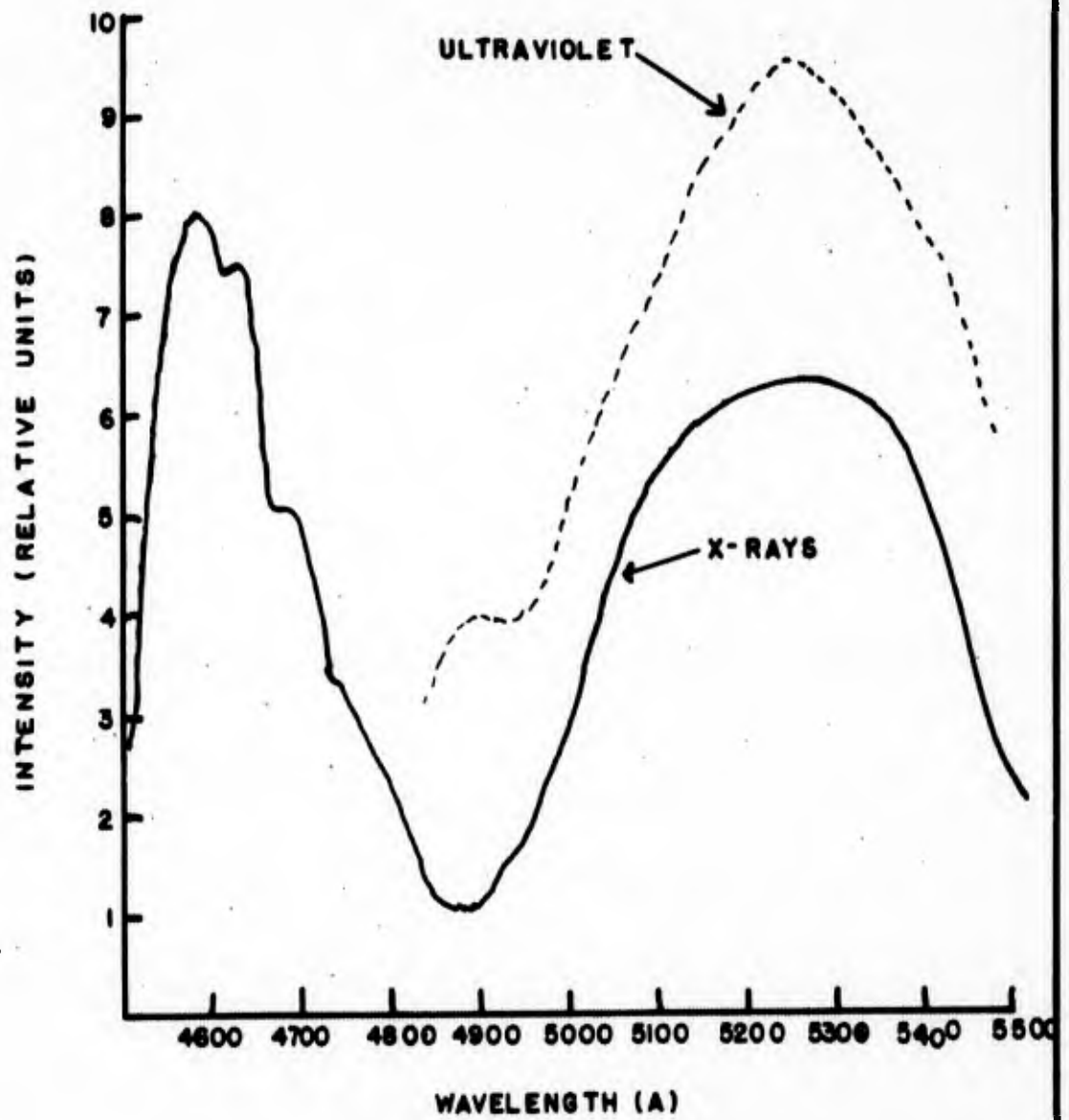


FIGURE 8 8 DENSITOMETER TRACES OF ZnSe  
FLUORESCENCE UNDER X-RAYS AND ULTRAVIOLET AT  
LIQUID NITROGEN TEMPERATURE

Such is not always the case. In some crystals the structured emission does not appear in either excitation case and the spectra is the same whether the crystal is excited with uv or x-rays. Differences in spectra with different exciting radiation are common in fluorescent materials.<sup>13</sup>

In crystals which do not have the structured edge emission, two other bands, one at  $0.46\mu$  and the other at  $0.45\mu$ , are often observed under x-ray stimulation. These bands generally do not appear together in the same crystal. The bands are observed also at  $4.2^{\circ}\text{K}$  under uv and are located at about  $0.45\mu$  and  $0.44\mu$  respectively. These latter bands arise from centers which are different from the edge emission centers observed by Reynolds. The  $0.45\mu$  band has been observed in a crystal which has the structured emission, a type II crystal, according to Reynolds.

Discussion. The bands observed at  $2.0\mu$  and  $2.2\mu$  in these crystals are very close to the bands reported by Avinor and Meijer<sup>3</sup> for vanadium activated ZnSe, and while Ag and Cu were found in the spectral analysis, no vanadium was detected. The excitation spectrum of the fluorescence observed here was not measured so that no further comparison is possible.

The observance of the intense edge emission at liquid nitrogen temperature under x-ray excitation while not under uv excitation can

be explained in several possible ways. First, surface contamination can contribute since the uv light is strongly absorbed on the surface while the x-rays are not. This effect would seem to be eliminated if the crystals were cleaved, however even cleaved surfaces give the effect shown in Figure 8. A second possible explanation is that the number of centers ionized by the deeply penetrating x-radiation is several orders of magnitude larger than the number of centers ionized by the strongly absorbed uv. A third possible explanation could be that the demarcation level<sup>17</sup> under uv excitation is below the defect level responsible for the fluorescence, hence the electron trapped at the defect is not in a ground state and available for recombination with a free hole with the emission of fluorescence radiation. (Note the model of a trapped hole and free electron is equally applicable.) Probably all three causes are contributing to the effect although it has been observed that the crystals used were of very high resistivity. No edge emission is observed in low resistivity "p" type ZnSe, which supports the demarcation line effect. However, since neither the defect responsible nor the conditions necessary and sufficient for observation of edge emission are known, the latter observation is not conclusive.

Displacement of the Selenium Atom

The native defects in ZnSe, zinc and selenium vacancies and interstitials, are most likely responsible for some of the fluorescence bands observed under bombardment. It is the object of this experiment to correlate the production of one particular fluorescence band with the creation of the selenium defect. Even though the atomic weights of zinc and selenium are fairly close together, it should be possible to observe distinct thresholds for their displacement, one at a lower energy representing displacement of the zinc atom and one at the higher energy representing displacement of the selenium atom. Such measurements have been made on CdS by Kulp and Kelly,<sup>10,11</sup> the sulfur displacement being observed at 115 kev and the cadmium atom displacement at 290 kev. It is reasonable to assume similar measurements can be made in ZnSe.

The experimental results which have led to the definition of the displacement energy of the selenium atom in ZnSe are presented in this section.

Displacement Data and Results. Figure 9 shows the initial curves of the fluorescence of a certain crystal of ZnSe under electron bombardment, which were taken at 350 kev,  $5.0 \mu\text{a}/\text{cm}^2$  ( $3 \times 10^{13}$  electrons/sec), at  $77^\circ\text{K}$  in the Van de Graaff Accelerator. Large peaks at  $0.46 \mu$  and  $1.6 \mu$  are observed as well as a small peak at  $1.0 \mu$ . There is also an

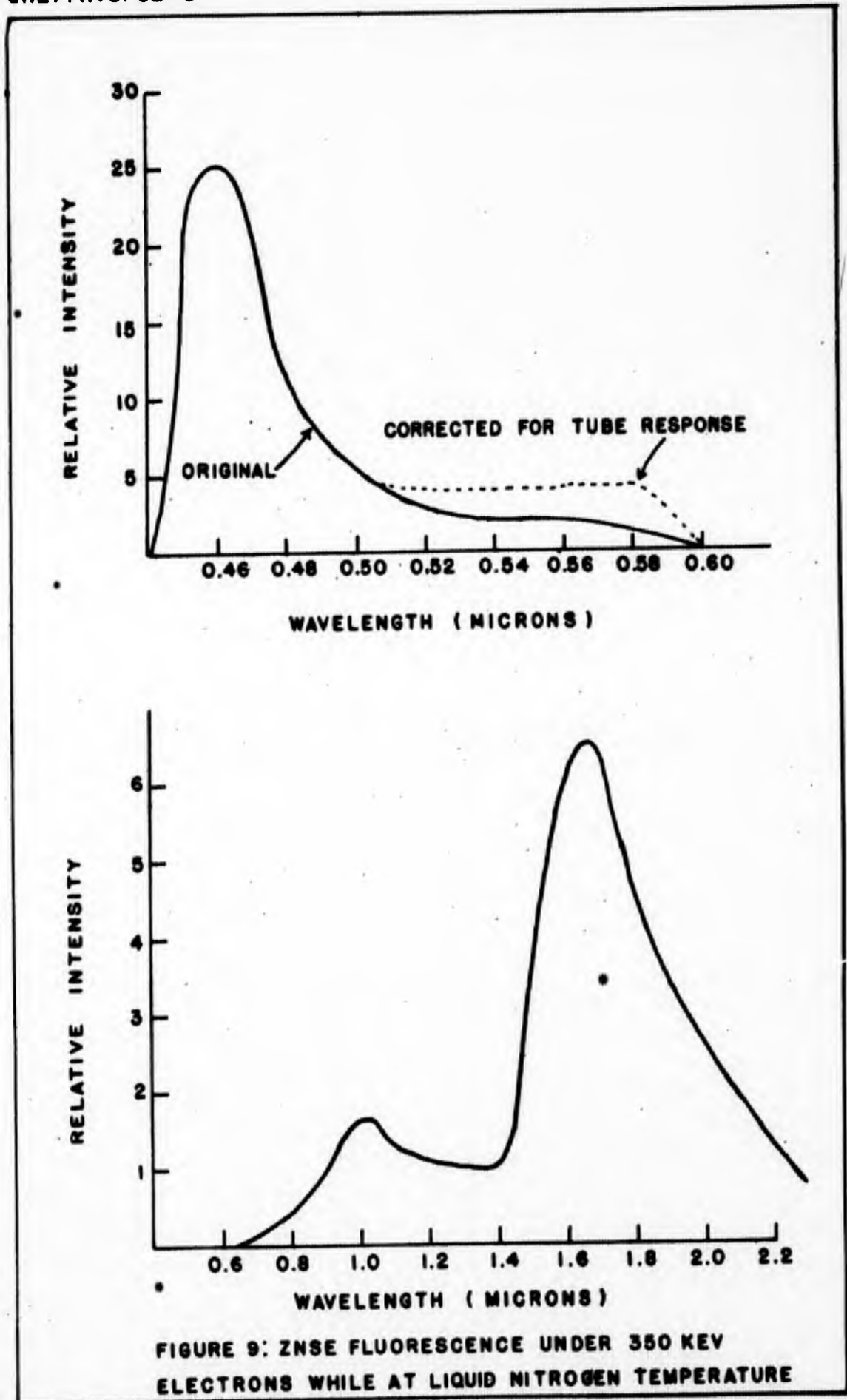


FIGURE 9: ZNSE FLUORESCENCE UNDER 350 KEV ELECTRONS WHILE AT LIQUID NITROGEN TEMPERATURE

obvious tailing off of the  $0.46\mu$  peak on the long wavelength side, which is evidence of possible  $0.49\mu$  and/or  $0.525\mu$  bands. The crystal was subsequently bombarded with  $10^{18}$  electrons/cm<sup>2</sup> at energies ranging from 350 kev to 400 kev at 300°K. Figure 10 shows the spectrum at the completion of this series. These bombardments indicated that a new band with a peak value of  $0.55\mu$  was being produced in this energy range at room temperature. When the electron beam was removed from the crystal for several hours, the crystal returned to its original fluorescence pattern indicating that the new band was unstable at room temperature. The infrared spectrum declined in intensity during these bombardments and was not further investigated. When bombardment was carried out at 77°K, one observes the intensity of the  $0.55\mu$  band to increase by a factor of 10 after  $3 \times 10^{16}$  electrons/cm<sup>2</sup> at 350 kev and even more rapidly at higher energies without any apparent saturation. The increased peak intensity can be plainly seen in Figure 11, which shows the fluorescence spectrum after  $3 \times 10^{17}$  electrons/cm<sup>2</sup> at 350 kev at 77°K. When compared to the original fluorescence of Figure 9 and the fluorescence after room temperature bombardment shown in Figure 10, one observes that liquid nitrogen temperature appears to be much more favorable for the growth of this band.

The intensity of the  $0.55\mu$  band as a function of bombardment

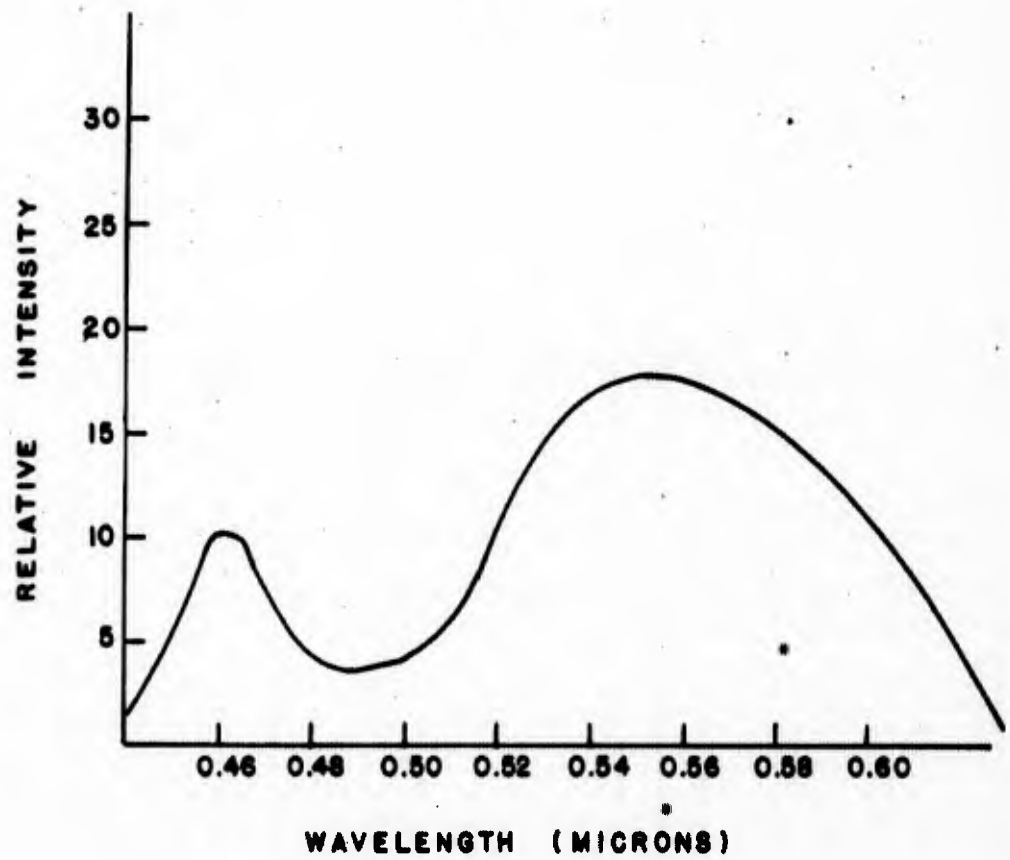


FIGURE 10: ZNSE FLUORESCENCE AFTER  $10^{18}$  ELECTRONS AT ENERGIES BETWEEN 350 KEV AND 400 KEV AT 300°K

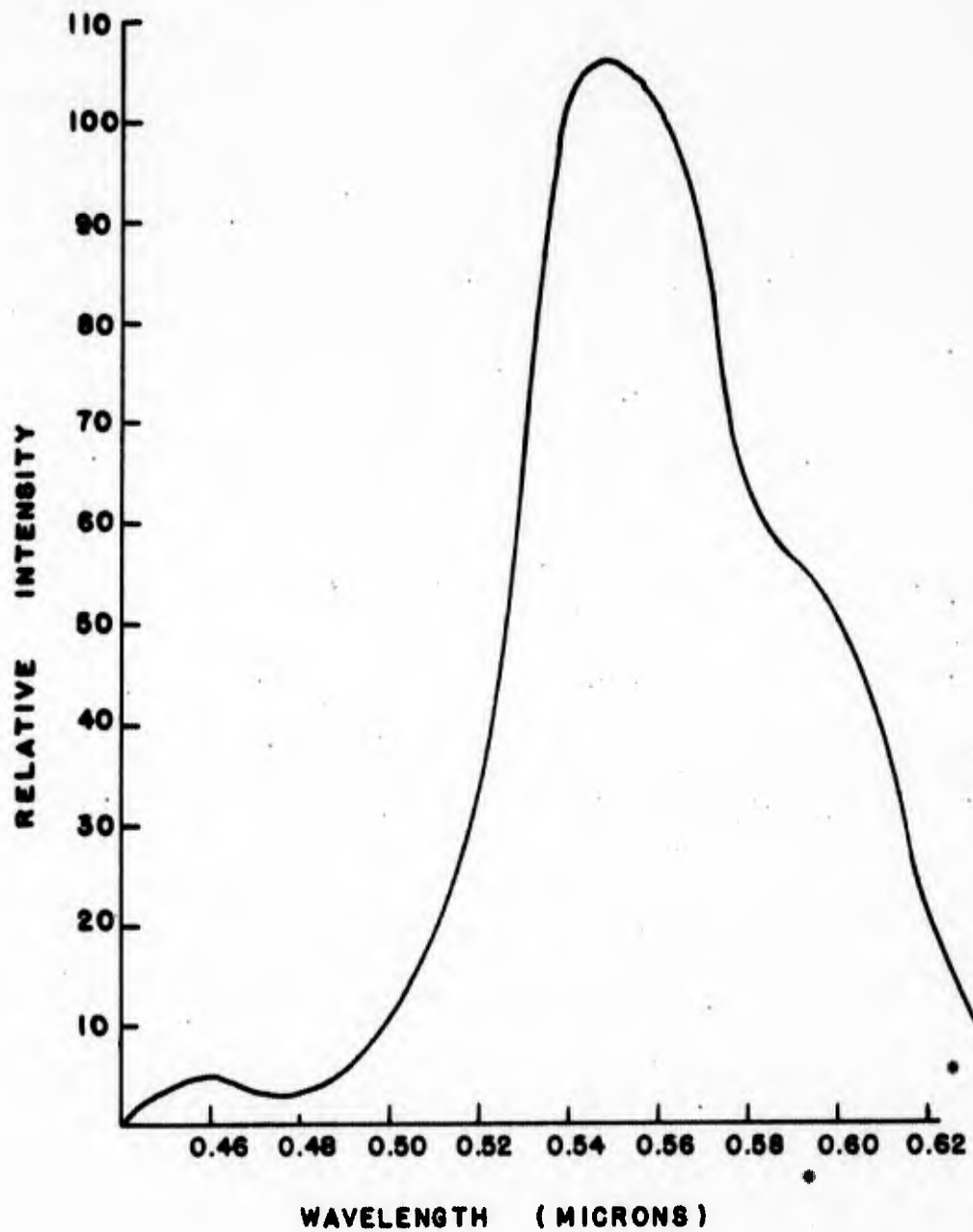


FIGURE II: ZNSE FLUORESCENCE AFTER  
 $3 \times 10^{17}$  ELECTRONS AT 350 KEV AT 77°K

time in the energy range between 225 kev and 500 kev is shown in Figure 12. It was observed that the growth rates of the  $0.55\mu$  band were very nearly linear at all energies except at 500 kev. This exception could be caused by the heating of the crystal, which possibly causes annealing or some saturation effect to take place. The rate of growth of the band at energies above 350 kev was so large that the spectra were taken at an energy of 275 kev, where the growth rate was small. The spectrum scan required about 7 minutes, which was approximately the time required for the peak intensity to double under 500 kev bombardment electrons. The increase in fluorescence intensity in the energy range of 250 kev to 300 kev was recorded after the crystal had been bombarded at a higher energy, at which the  $0.55\mu$  peak could clearly be identified. This was done to differentiate between the growth of the  $0.55\mu$  band and the growth and decline of adjacent peaks. The growth of the  $0.525\mu$  band near the threshold made low intensity peak resolution difficult. The growth rate of the  $0.55\mu$  band can be observed without high energy bombardment by observing a shift in the peak value of the broad  $0.525\mu - 0.55\mu$  complex. The shift from  $0.525\mu$  to  $0.55\mu$  occurs very slowly at energies between 250 kev and 300 kev requiring long term bombardment for a complete shift. The  $0.46\mu$  band also frequently overlapped the  $0.55\mu$  band

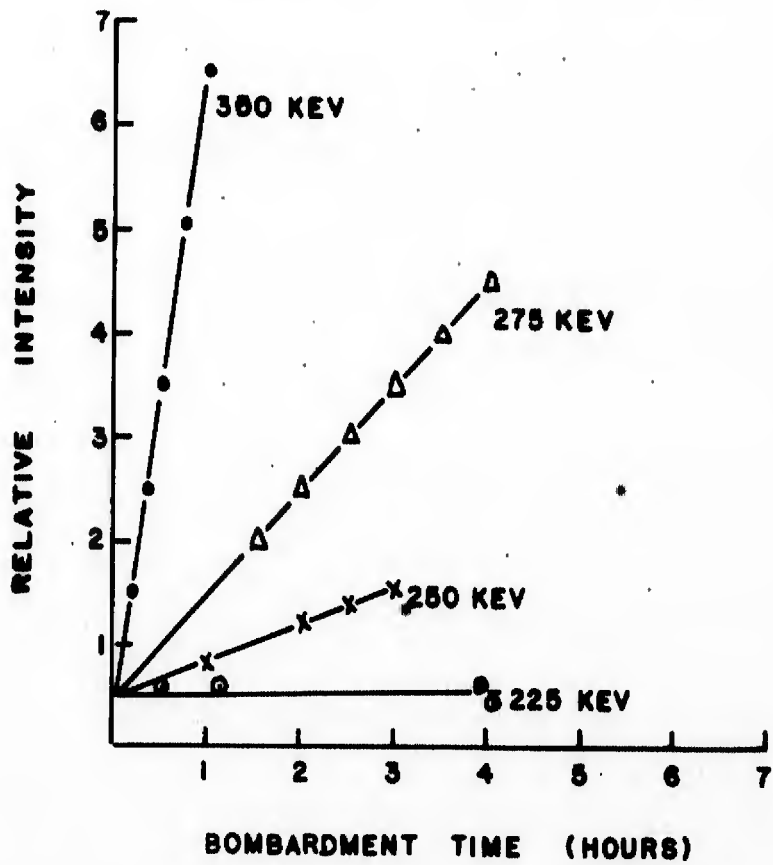
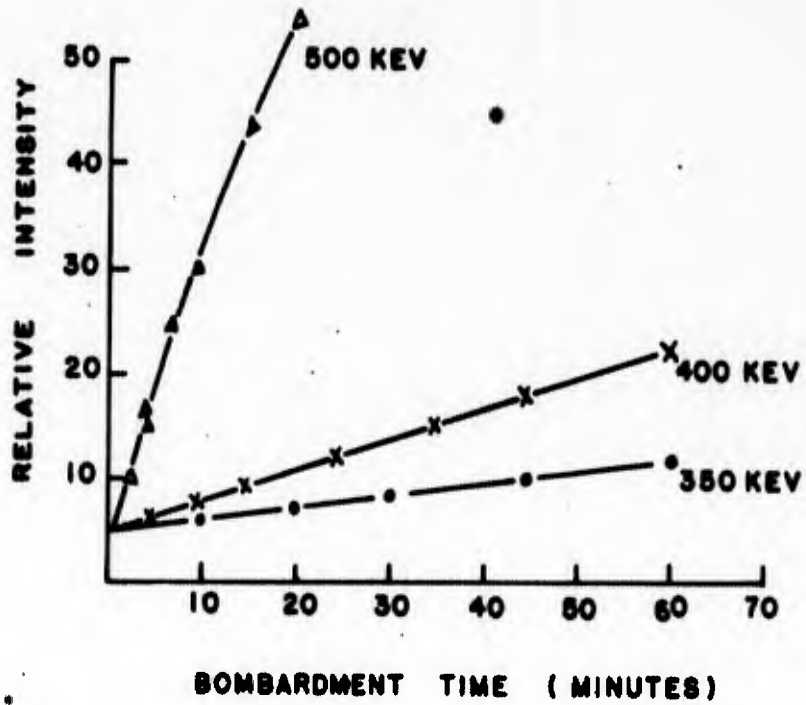


FIGURE 12: THE RATE OF GROWTH OF THE 0.550 MICRON BAND AT VARIOUS ENERGIES AS A FUNCTION OF BOMBARDMENT TIME

which precluded seeing small changes in the  $0.55\mu$  band peak.

Figure 13 shows the rate of growth of the  $0.55\mu$  band as a function of the electron energy. The linear portion of the curve shows the same steep rise in growth rate that would be expected from the sharp increase in the cross-section shown in Figure 1. One can conclude from Figure 12 and 13 that the threshold must be in the range between 225 kev and 250 kev. The slow growth of the fluorescence at 250 kev is readily evident in Figure 14. The solid line shows the initial fluorescence at  $77^{\circ}\text{K}$ . As bombardment is continued for  $3 \times 10^{17}$  electrons/cm<sup>2</sup>, the fluorescence changes to the dotted line in Figure 14. The bombardment time required for this small change was 5 1/2 hours.

The temperature dependence of this fluorescence band is shown in Figure 15. The peak fluorescence of the band was followed while the temperature was raised from  $77^{\circ}\text{K}$  while being bombarded with 275 kev electrons. It was noted that upon recooling to  $77^{\circ}\text{K}$  that the fluorescence peak did not return, as the infrared band peaks have been observed to do under similar conditions. To further investigate this phenomena, an isochronal experiment was performed, which consists of raising the temperature of the crystal a few degrees while under electron bombardment and holding it at this temperature for some arbitrary length of time and then recooling to obtain a spectrum.

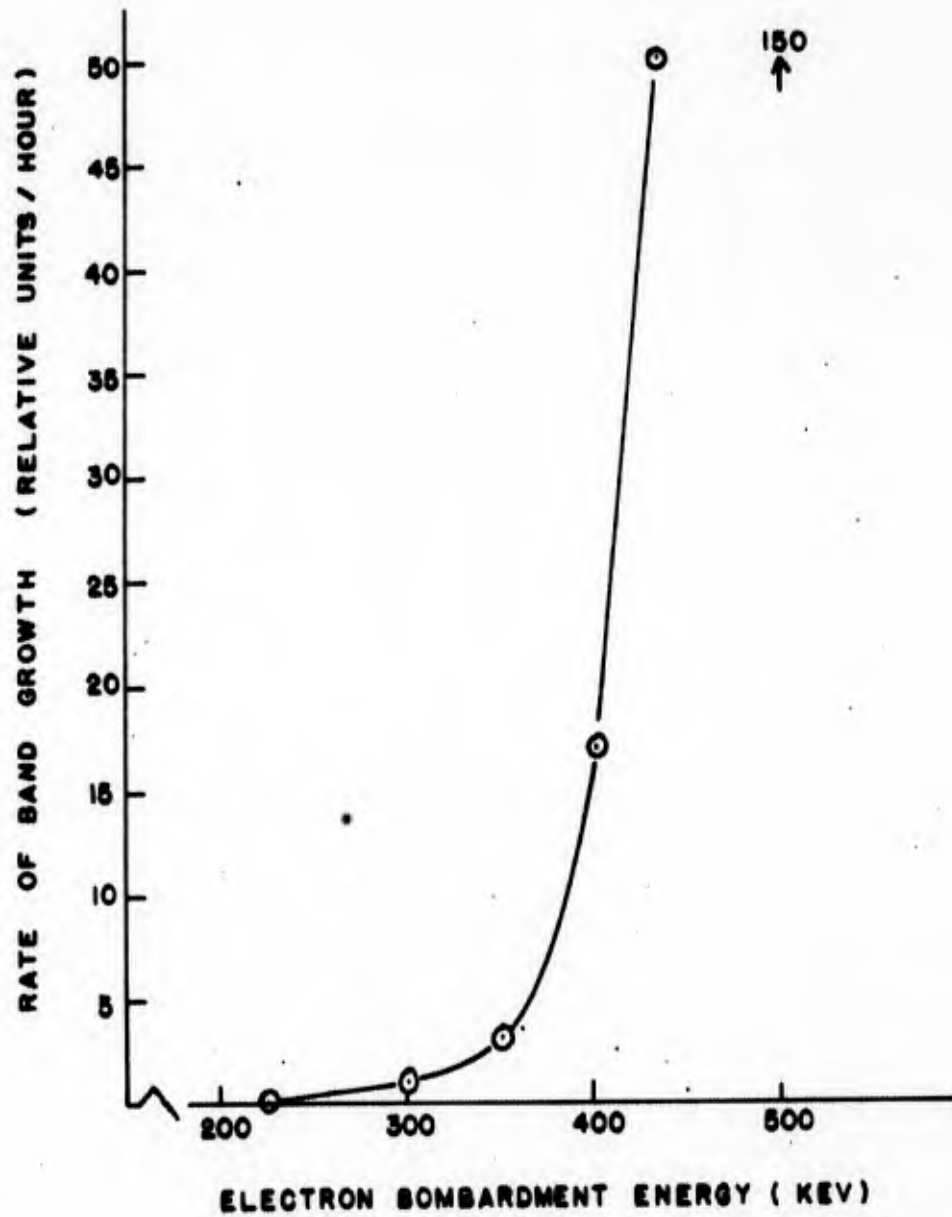


FIGURE 13: THE RATE OF GROWTH OF THE 0.550 MICRON BAND AS A FUNCTION OF BOMBARDMENT ENERGY

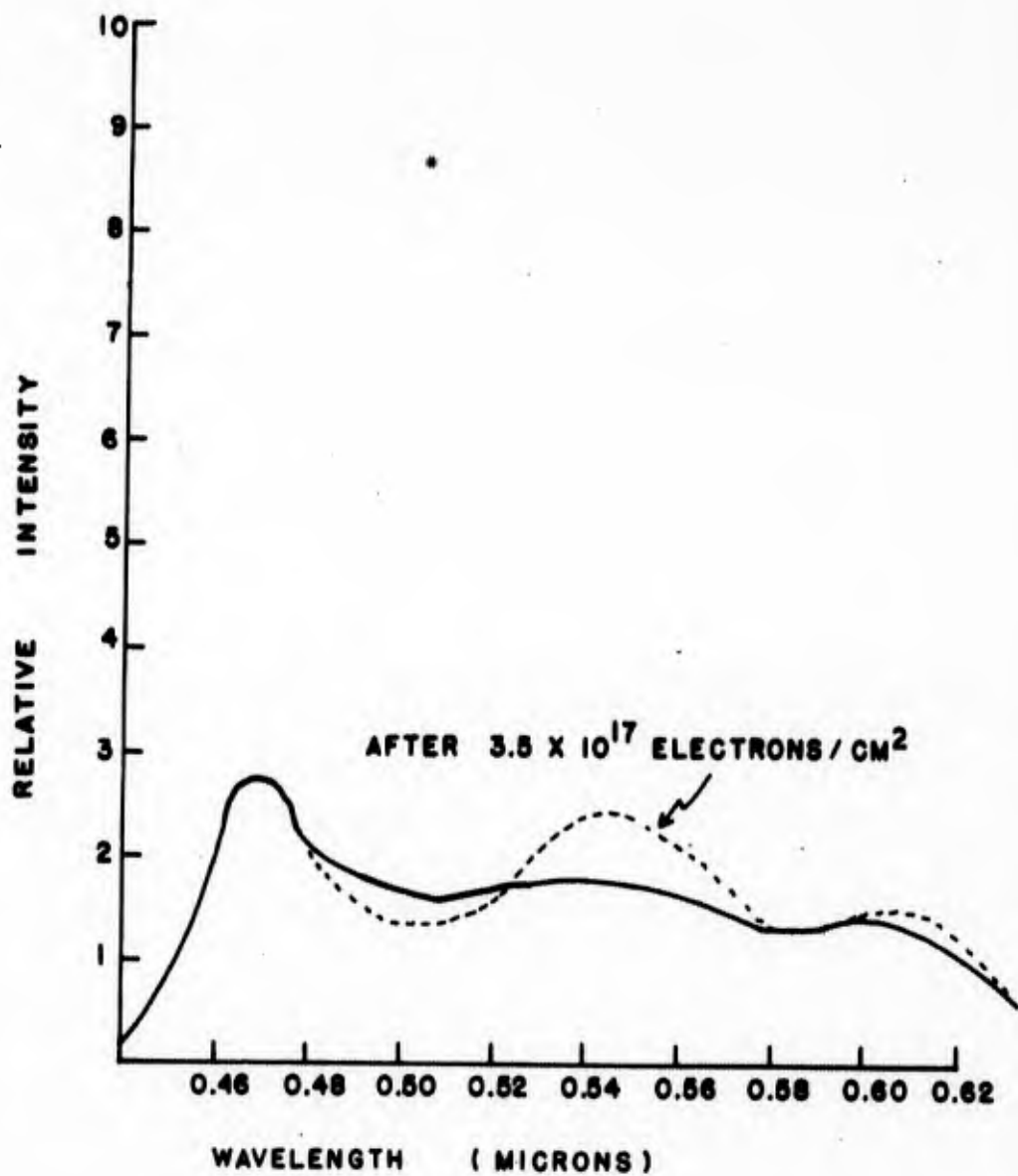


FIGURE 14: THE FLUORESCENCE GROWTH OF THE 0.550 MICRON BAND UNDER 250 KEV ELECTRONS AT LIQUID NITROGEN TEMPERATURE

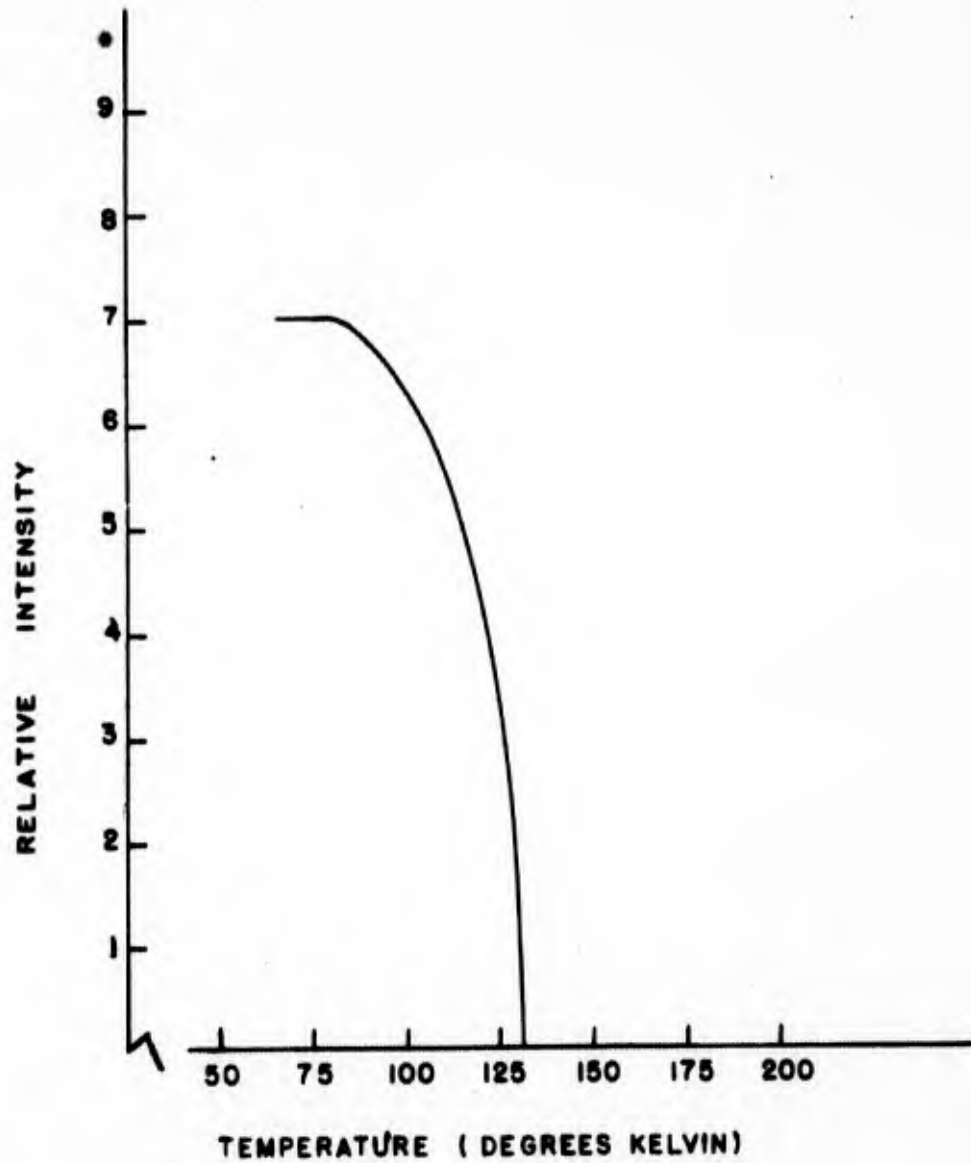


FIGURE 15: THE TEMPERATURE DEPENDENCE OF THE 0.550 MICRON BAND WHILE UNDER 275 KEV BOMBARDMENT ELECTRONS

The peak temperature is increased on each successive cycle until the temperature at which the fluorescence completely disappears is defined. The results of this experiment showed that the fluorescence peak decreased in intensity starting at about 85°K with complete disappearance of the band at about 130°K.

Discussion. This experiment shows that the intensification of the 0.55 $\mu$  band in ZnSe under electron bombardment has a threshold between 225 kev and 250 kev. The necessity of conducting this experiment at liquid nitrogen temperature is borne out by the fact that the defect responsible for this band is very sensitive to temperature changes as shown in Figure 15. The instability of the fluorescence above 77°K indicates that this defect is a simple one, that is, it does not depend on a second impurity or another defect for its formation. A similar unreported threshold in ZnSe for the growth of the 0.525 $\mu$  band has been observed in the vicinity of 200 kev.<sup>21</sup> Therefore, since a definite threshold characteristic is exhibited, one can assume the 0.55 $\mu$  band to be a product of atom displacement of the heavier element and not a redistribution of electrons over the existing defects. The threshold observed here is for the displacement of the selenium atom from its lattice point, while the threshold near 200 kev is associated with the zinc displacement. For convenience, a value of

$240 \pm 10$  kev is taken as the displacement energy. This corresponds to a maximum energy transfer to the selenium atom of 8.2 ev.

It is interesting to note that the shape of the curve in Figure 13 compares quite favorably to the probability of displacement curve for germanium reported by Loferski and Rappaport.<sup>14</sup> The fact that this does not coincide with the theoretical cross-section shown in Figure 1 is to be expected. The displacement of an atom from the lattice does not take place at a definite energy. The vibrational motion of the atom and the isotope concentrations and the different ionization states of the lattice atoms contribute to the broadening of the displacement interval. The growth rates observed near the displacement energy, most probably as a result of these factors, point out the sensitivity of the electron beam probe for this type of analysis.

On the basis of the calculated cross-section at 350 kev and an electron flux of  $5 \mu\text{a}/\text{cm}^2$ , the reaction rate, which is assumed to be equal to the atom displacement rate, is approximately  $10^{16}$  selenium atom displacements/hour- $\text{cm}^2$ . The actual area of the particular crystal was about  $4 \text{ mm}^2$  as compared to the cross-section area of the electron beam of about  $75 \text{ mm}^2$ . If we consider the electron flux/unit area to be uniform, a total of about  $10^{14}$  defects/hour are created in the crystal. The change in intensity observed at 350 kev from Figure 11 resulting from a 5 hour bombardment is nearly 100 times the

detectable amount in a fluorescence change. Therefore, it is possible to observe a change in defect population of the order of  $10^{12}$  to  $10^{13}$  by observing a change in the fluorescence spectrum.

The temperature sensitivity of the  $0.55\mu$  band as shown in Figure 15 as well as the disappearance of the band following a temperature cycle to room temperature indicate that this effect could be caused by either a redistribution of electrons over existing defects or an annealing of the causing defect. If the destruction of this band is due to the redistribution of electrons over existing defects, the regrowth of the  $0.55\mu$  band should not exhibit a threshold property. However, each time the band was destroyed, it was necessary to bombard the crystal above 225 keV at  $77^{\circ}\text{K}$  to restore the  $0.55\mu$  band. Thus, the annealing process is most likely responsible for this effect.

An attempt was made to differentiate between the selenium interstitial and vacancy as the causing defect for the fluorescence band by the interstitial diffusion experiment shown schematically in Figure 16. The crystal was overlaid with a few micrograms/cm<sup>2</sup> of selenium. Bombardment with 100 keV electrons at  $2.0 \mu\text{a/cm}^2$  for 4 hours did not produce the  $0.55\mu$  band. Additional bombardment at 120 keV,  $2.0 \mu\text{a/cm}^2$  for 6 hours did not produce any change in the fluorescence.

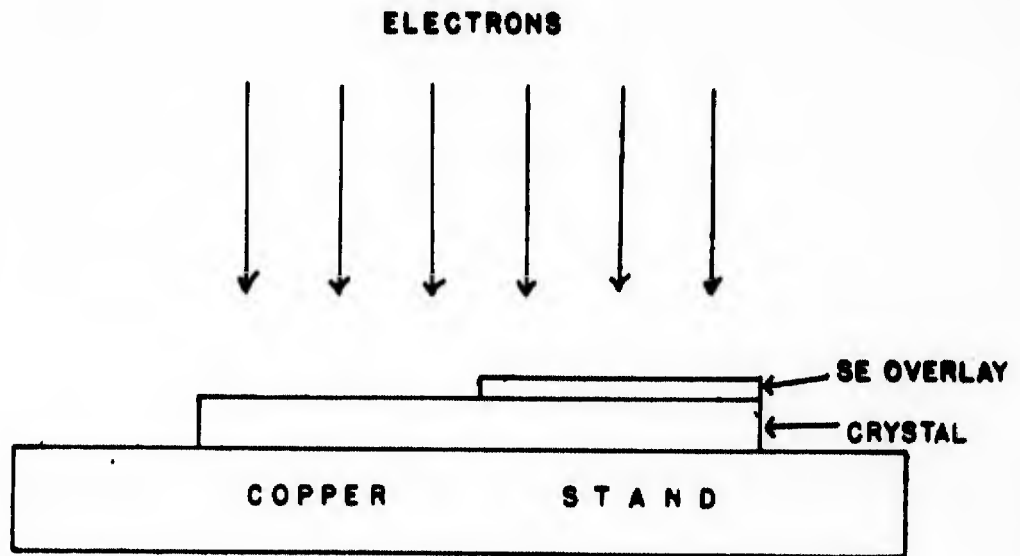


FIGURE 16: SCHEMATIC ARRANGEMENT OF THE INTERSTITIAL DIFFUSION EXPERIMENT ON ZINC SELENIDE

Although one may postulate the selenium vacancy to be the causing defect, the results of this overlay experiment are not conclusive in this respect. However, the high mobility of the responsible defect observed in the sharp temperature dependency in the annealing experiment in addition to the results of the overlay experiment indicated that the  $0.55\mu$  band is most probably caused by the selenium vacancy.

VII. CONCLUSIONS

The low-energy electron beam provides a unique means with which the analysis of crystal fluorescence can be made. It not only provides a discrete energy source for producing radiation damage, but also the ionization of these defects, which is necessary for their detection. The threshold energy measurements in CdS and ZnSe are analytical in nature and show conclusively that there is an energy dependent relation between particular fluorescence bands and the defects found in the crystal. Many other factors may be involved in these measurements, but are apparently well behaved and, in general, do not preclude the reproducibility of these experiments. The electron beam, by comparison to any other method of radiation damage, holds these parameters to a minimum so that defects may be singled out for examination. The resulting information is limited only by ones ingenuity and ones ability to analyze the data.

The fluorescence band-defect relationships for zinc selenide are by no means solved. This work has just begun the long series of experiments on this compound that are necessary in order to have an intimate knowledge of just a few of its basic characteristics. Additional experiments are plainly evident at this time. The study of the infrared spectrum out to  $5.0\mu$  could be examined with an InSb infrared

detector, which would provide a much more complete range of optical interest. A threshold for the production of the  $0.525\mu$  band has been observed at about 200 kev and has been assumed to be the displacement energy required for the zinc defect. Overlay experiments have not been conclusive in verifying this observation. All of the fluorescence bands that were observed in ZnSe crystals change under electron bombardment; some are destroyed with no apparent threshold, while others show no definite pattern. As yet, there is no way to identify which one of the several possible states of ionization a defect may be in to cause fluorescence. Photoconductivity and Hall measurements will certainly add strength, and may ultimately verify, the theory of interstitial-vacancy production at various thresholds in zinc selenide. All of the fluorescence bands must some day be explained in terms of defects, impurities, or lattice rearrangements. These problems pose an interesting challenge for further study in the field of radiation damage.

Bibliography

1. Anders, William. Temperature Dependence of Line Structure of CdS Edge Emission. Thesis. Air Force Institute of Technology: May 1962.
2. Aven, M., et al. "Some Electrical and Optical Properties of ZnSe." Journal of Applied Physics, 32: pp 2261-2265 (October 1961).
3. Avinor, M., and G. Meijer. "Excitation Spectra of Vanadium-Activated Zinc and Cadmium Sulfide and Selenide Phosphors." Philips Research Report 15. Eindhoven, Netherlands: Philips Research Laboratory, June 1960.
4. Bube, R. H. "Temperature Dependence of Band-Gap in CdS, CdSe, ZnS, ZnSe." Physics Review, 98: 431 (1955).
5. Dreeben, A. B., et al. Investigation of Carrier Injection Electroluminescence. Scientific Report #1. Princeton, New Jersey: RCA, 1961.
6. Evans, R. D. The Atomic Nucleus. New York: McGraw-Hill, 624 (1955).
7. Greene, L. C., and D. C. Reynolds, et al. "Method for Growing Large CdS and ZnS Single Crystals." Journal of Chemical Physics, 29: 1375 (1958).
8. Korneeva, I. V., V. V. Sokolov, and A. V. Nooselova. "Vapor Pressure of Selenides of Zn and Cd." Zhur. Heorg. Kim., 5: 241-245 (1960).
9. Kroger, F. A. "Luminescence and Absorption of ZnS and CdS and Their Solid Solutions." Physica I, 1; 1-12 (1940).
10. Kulp, B. A., and R. H. Kelley. "Displacement of the Sulfur Atom in CdS by Electron Bombardment." Journal of Applied Physics, 31: 1057-1061 (June 1960).
11. Kulp, B. A. "Displacement of the Cadmium Atom in Single Crystal CdS by Electron Bombardment." The Physical Review, 125: 1865 (March 15, 1962).

12. - - - . "Effect of Electron Bombardment on the Near-Infrared Fluorescence of Single Crystal CdS." Journal of Applied Physics, 32: 1966-1969 (October 1961).
13. Leverenz, H. W. An Introduction to Luminescence of Solids. New York: John Wiley and Sons, Inc. 1950.
14. Loferski, J. J., and P. Rappaport. "Displacement Thresholds in Semiconductors." Journal of Applied Physics, 30: 1296-1299 (August 1959).
15. Reynolds, D. C., and L. C. Greene. "Production of Green Emission in CdS by Proton Bombardment." American Physical Society Bulletin: 3, 108 (1958).
16. Reynolds, D. C., L. S. Pedrotti, and O. W. Larson. "Edge Emission in Zinc Selenide Single Crystals." Journal of Applied Physics, 32: 2250 (1961).
17. Rose, A. "Performance of Photoconductors." in Photoconductivity Conference; John Wiley and Sons, Inc, 1956.
18. Seitz, F., and J. S. Koehler. "Displacement of Atoms During Irradiation." in Solid State Physics, Vol. II. New York: Academic Press, 1956.
19. Vineyard, G. H. "Radiation Effects in Inorganic Solids." Discussions of the Faraday Society, 31: 7-23 (1961).
20. Zholdevich, G. A. "The Optical and Photoelectric Properties of Zinc Selenide and Telluride." Soviet Physics--Solid State, 2: 115 (June 1960).
21. Unpublished Experiments by Kulp and Detweiler, to be published.

Vita

Robert milan Detweiler [REDACTED]

[REDACTED] spent his childhood in Zeigler, Illinois where he received his early education up through high school. His first year of college was taken at Oberlin College, Ohio in preparation for the United States Naval Academy. The following four years were spent at the Academy where he had the honor to row on the Olympic Champion Crew Team in 1952. After receiving his degree of Bachelor of Science in Electrical Engineering from the Academy, he received a commission in the Air Force and went through pilot training at Malden, Missouri and at Enid, Oklahoma. He received his wings in 1954 followed by an assignment to Ellington AFB, where he flew in the navigator training program. In 1956 he spent a short tour of duty as the Air Force advisor to Midshipmen at the Naval Academy before being sent to Orly Air Base, France as an instructor pilot. A year later, he was selected to be an aide-pilot for General Leon Johnson, at that time the Air Deputy for SHAPE. In 1960 he was transferred back to the United States to attend the Air Force Institute of Technology to obtain a master's degree in Nuclear Engineering. His assignment from this school is in the Aeronautical Research Laboratories, where he will be working in the field of radiation damage.

[REDACTED] [REDACTED]  
[REDACTED]

This thesis was typed by Miss Catherine Horn and Mrs. Joanne Major.

**UNCLASSIFIED**

**UNCLASSIFIED**